UAVSAR Applied to Volcanoes

UAVSAR
Uninhabited Aerial Vehicle Synthetic Aperture Radar

Paul Lundgren, Jet Propulsion Laboratory, California Institute of Technology

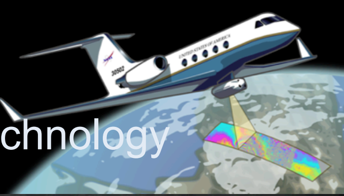

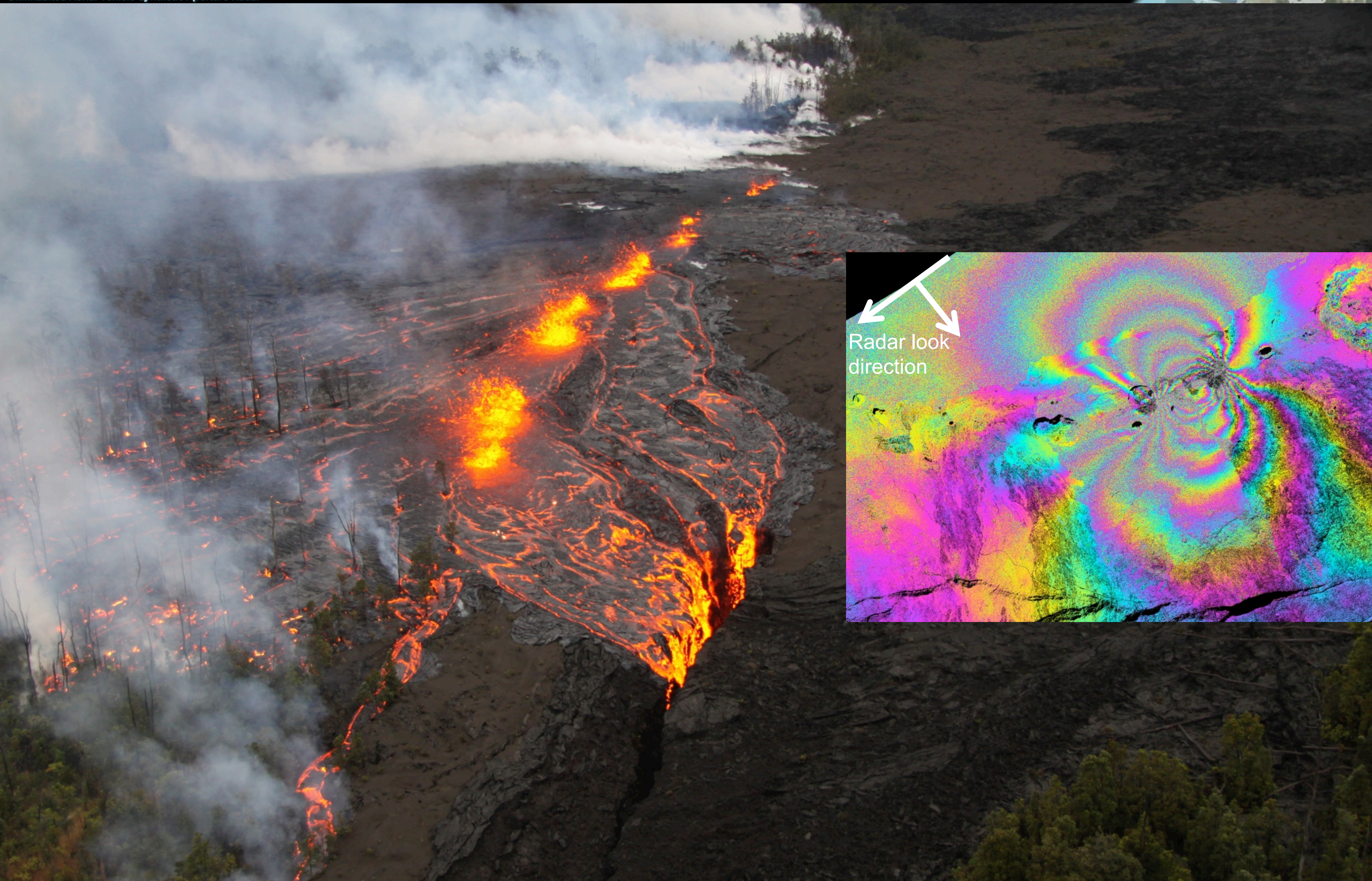

UAVSAR
Uninhabited Aerial Vehicle Synthetic Aperture Radar

Why UAVSAR?

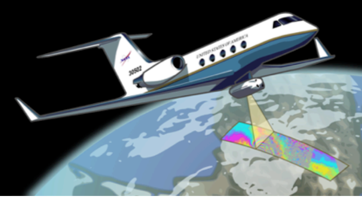

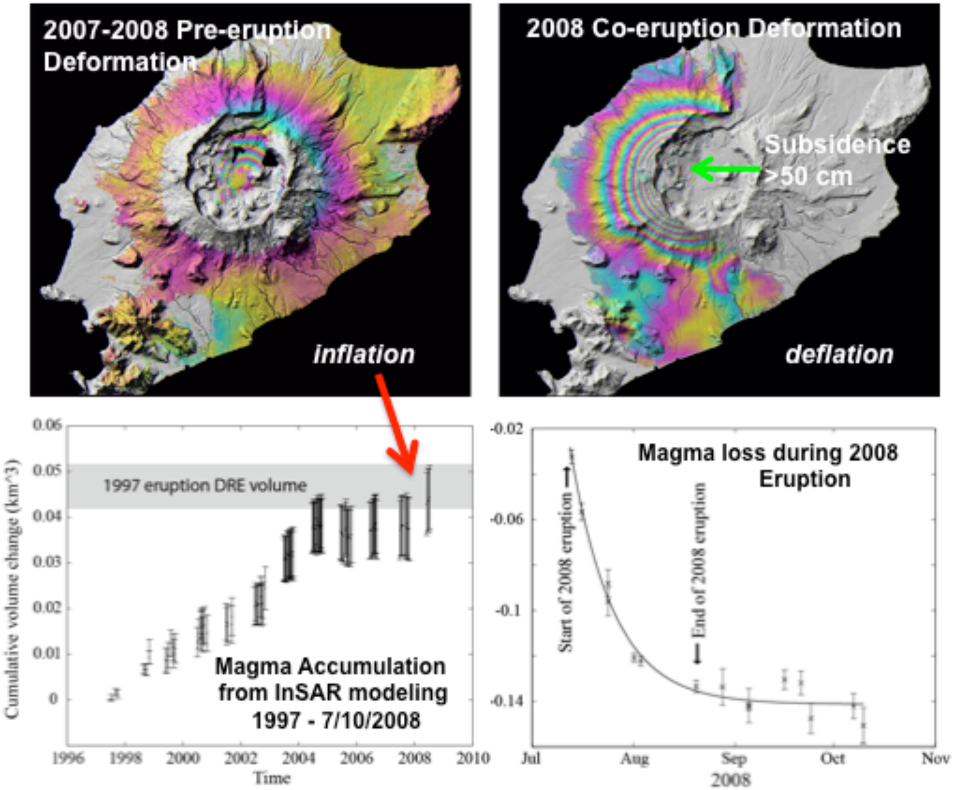

Satellite InSAR data of Okmok volcano Alaska illustrating the inter-annual build-up to the 2008 eruption and the larger 2008 co-eruption deflation. *Left top*, post-1997 eruption volume change and ESA Envisat interferogram showing the 10-15 cm inflation in prior year (lower left) to the July 13, 2008 Okmok, Aleutians eruption (max VEI ~4). *Right* , InSAR data and volume change decay plot for the months following the initial eruption. [*Lu et al.*, 1998, 2005a, 2010; *Lu and Dzurisin*, 2010].

Satellite data (figure on right) can provide global coverage at fixed repeat intervals (depending on satellite).

UAVSAR is deployed annually (in current study) with the possibility to return for temporally dense observations in the event of a significant volcano eruption crisis.

UAVSAR Volcanoes (2009-2011)

UAVSAR
Uninhabited Aerial Vehicle Synthetic Aperture Radar

UAVSAR acquired under 1st phase of funding (2009-2011)

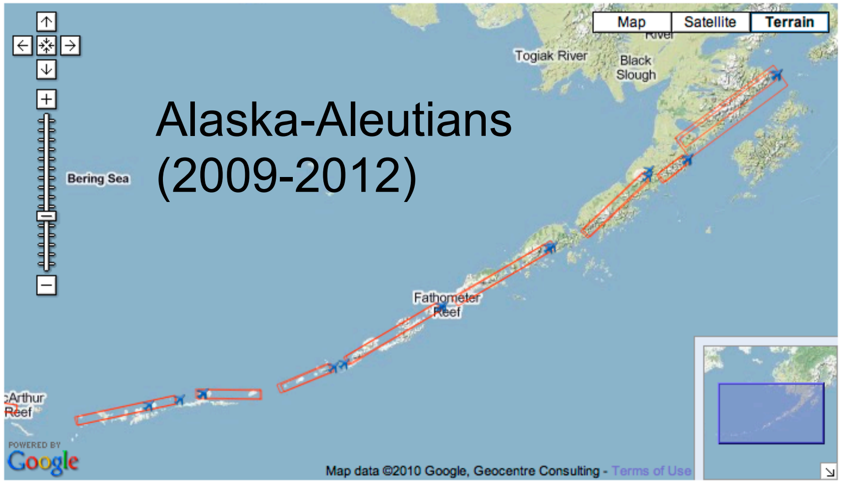

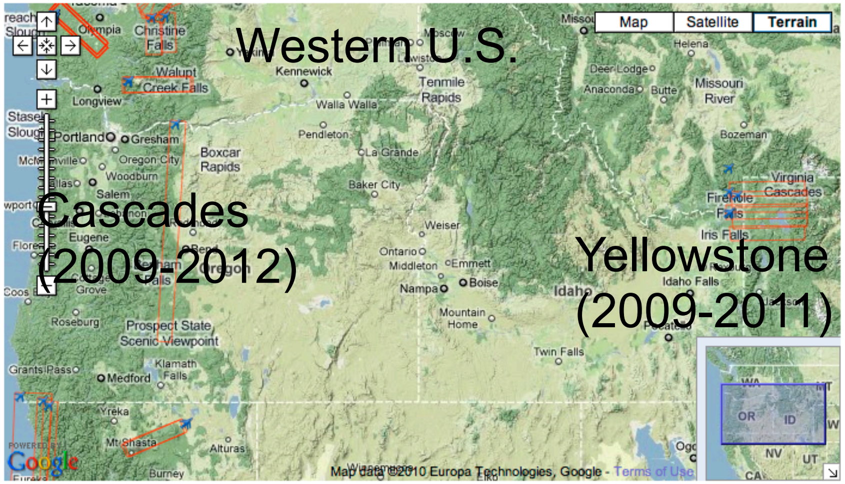

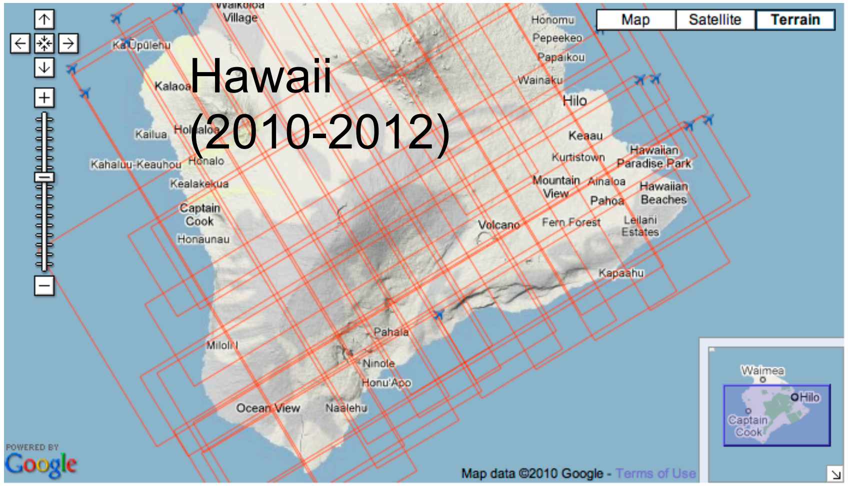

Pacaya Volcano Guatemala

2010-2011 UAVSAR data

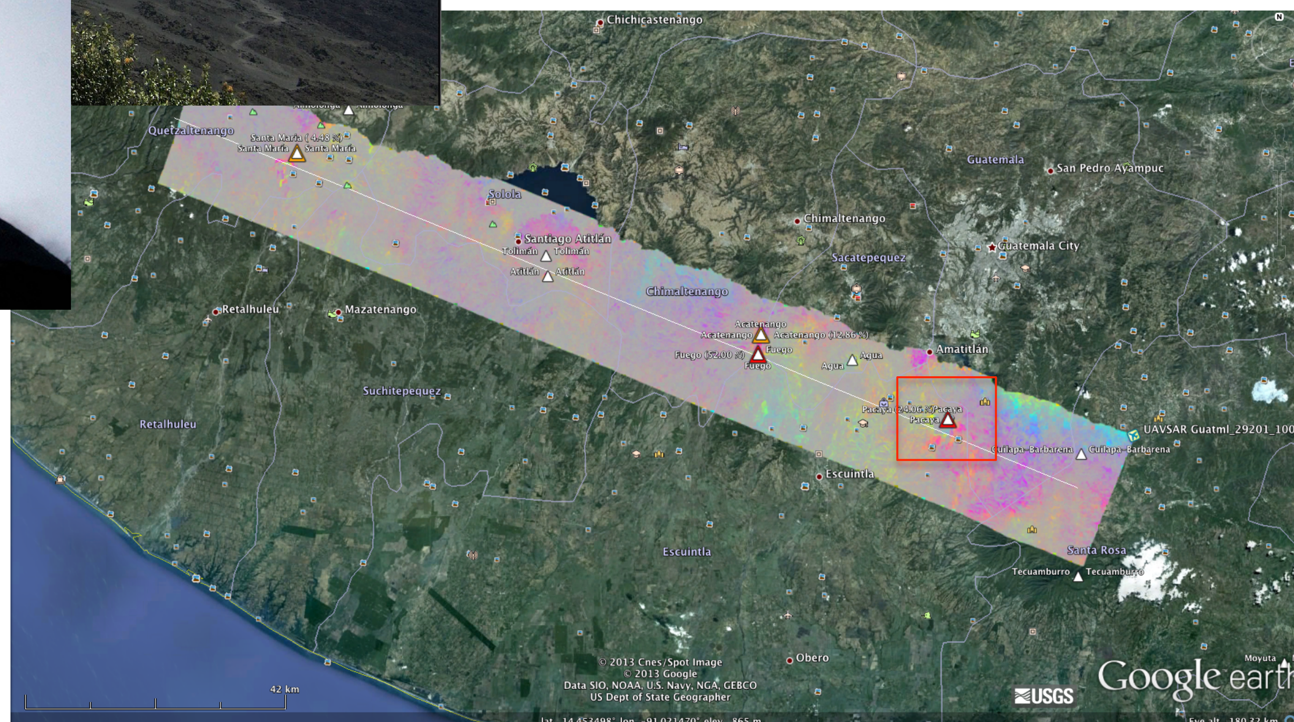

UAVSAR

Uninhabited Aerial Vehicle Synthetic Aperture Radar

Pacaya Volcano Guatemala

Slope instability?
(spans May 2010 eruption)

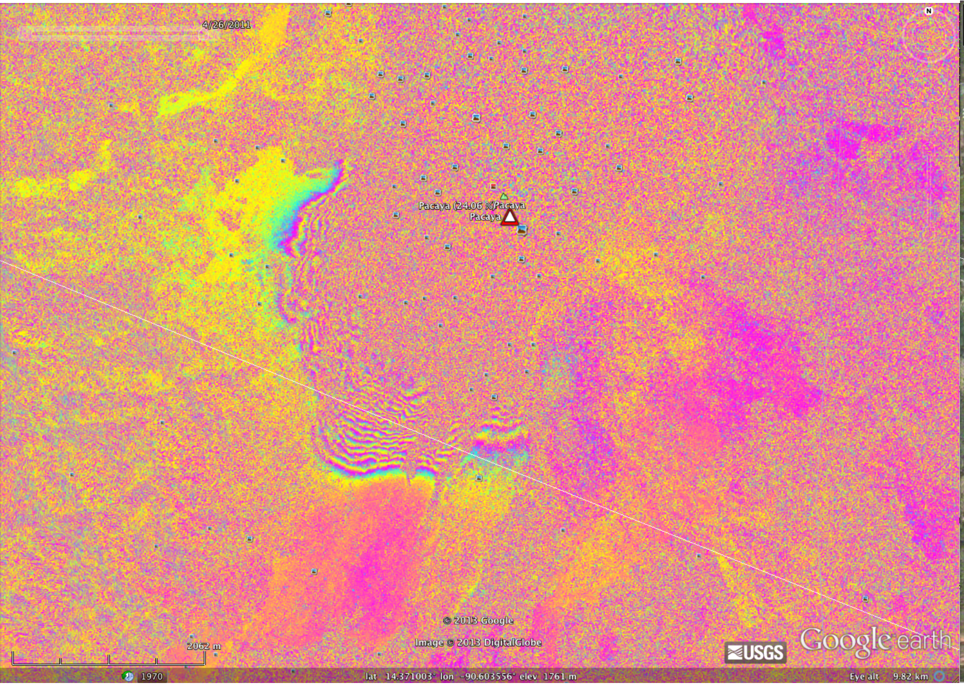

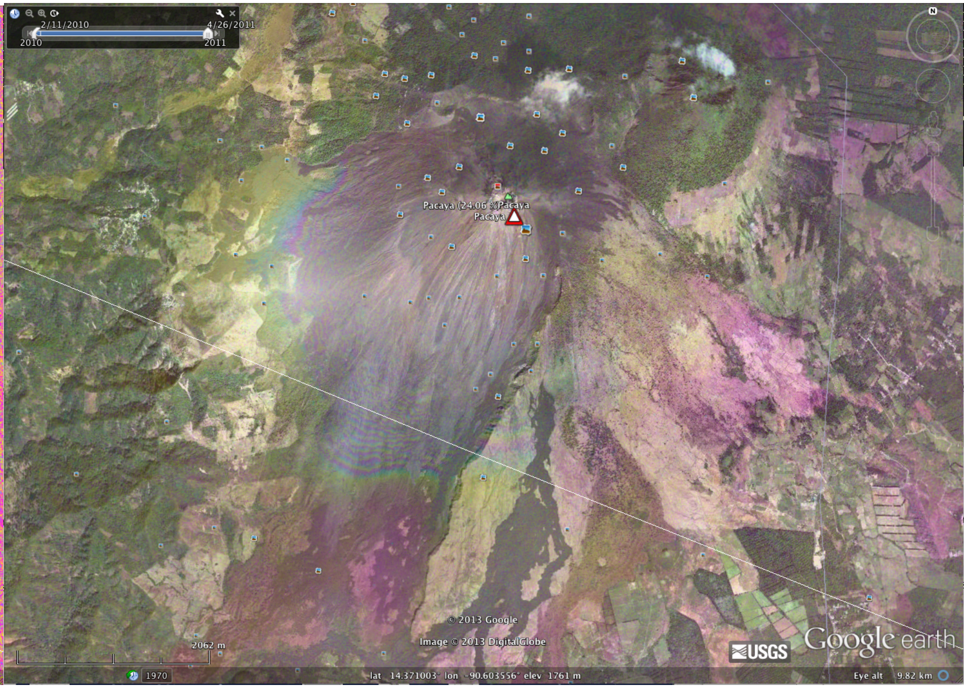

2010-2011 UAVSAR interferogram

UAVSAR
Uninhabited Aerial Vehicle Synthetic Aperture Radar

Pacaya Volcano Guatemala

2010/01/29-2010/02/11
UAVSAR data

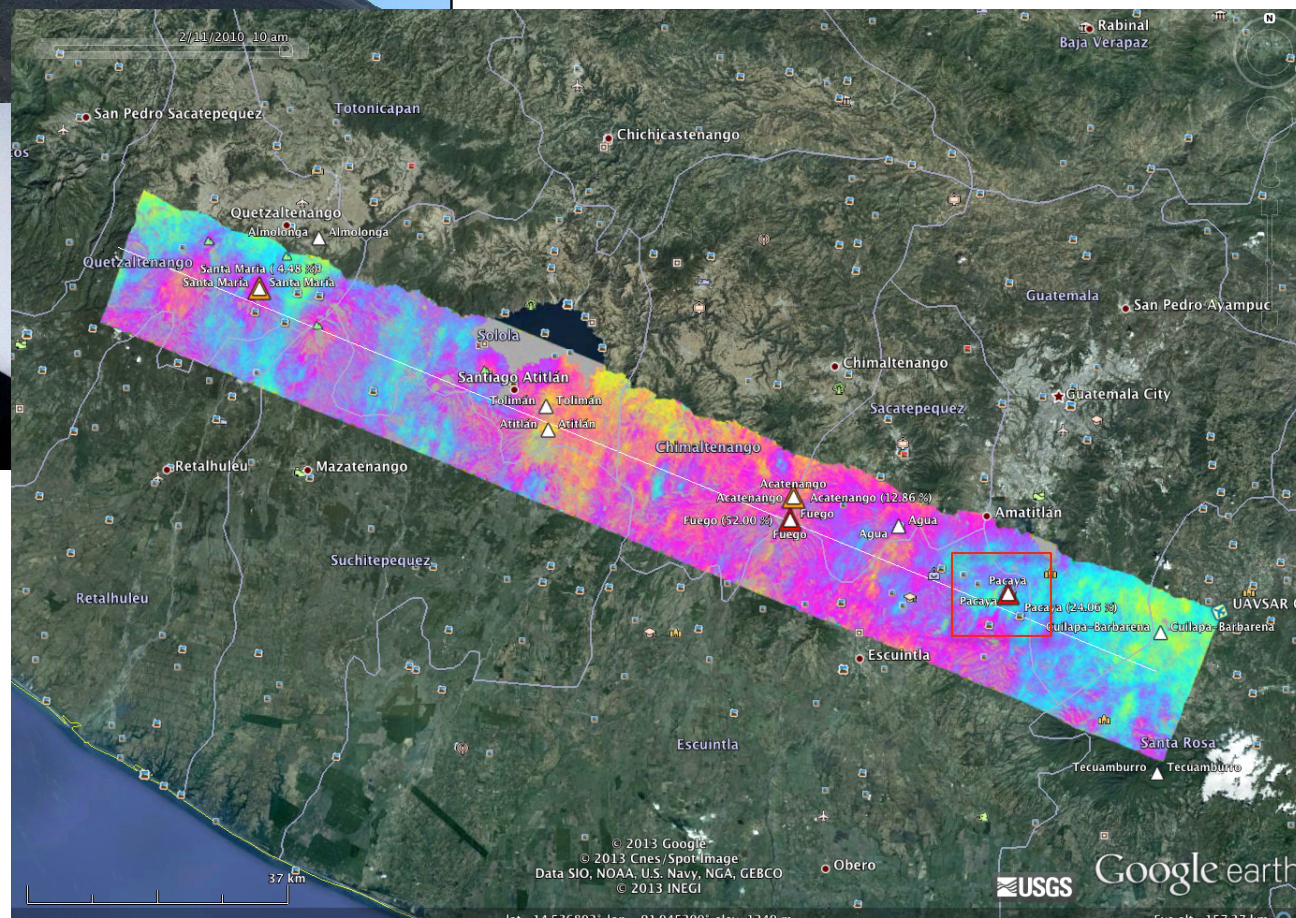

Pacaya Volcano Guatemala

UAVSAR
Uninhabited Aerial Vehicle Synthetic Aperture Radar

Slope instability?
(~2 week interferogram)

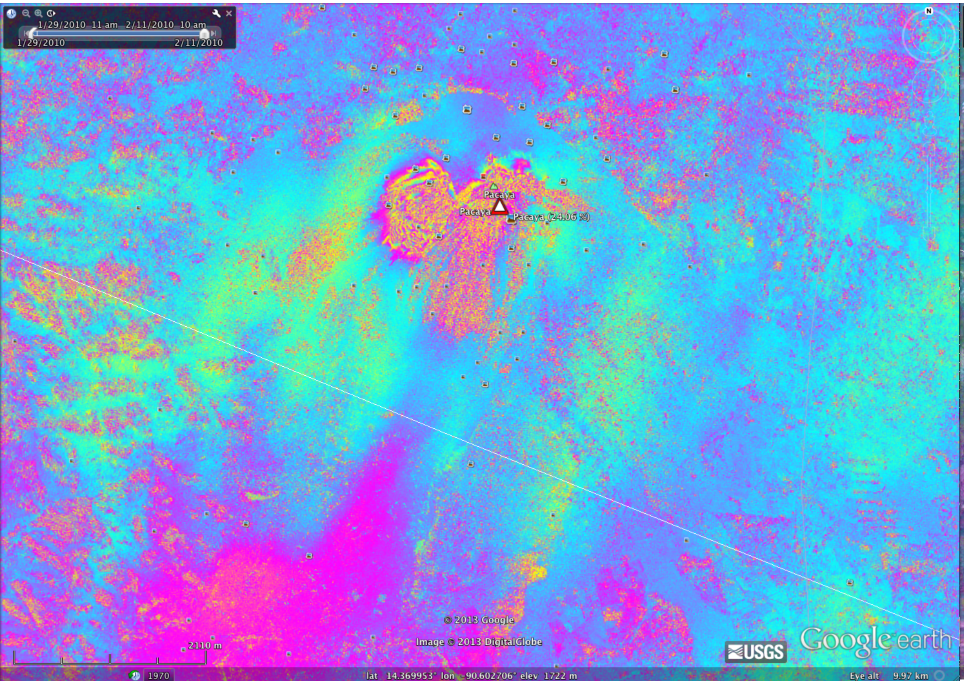

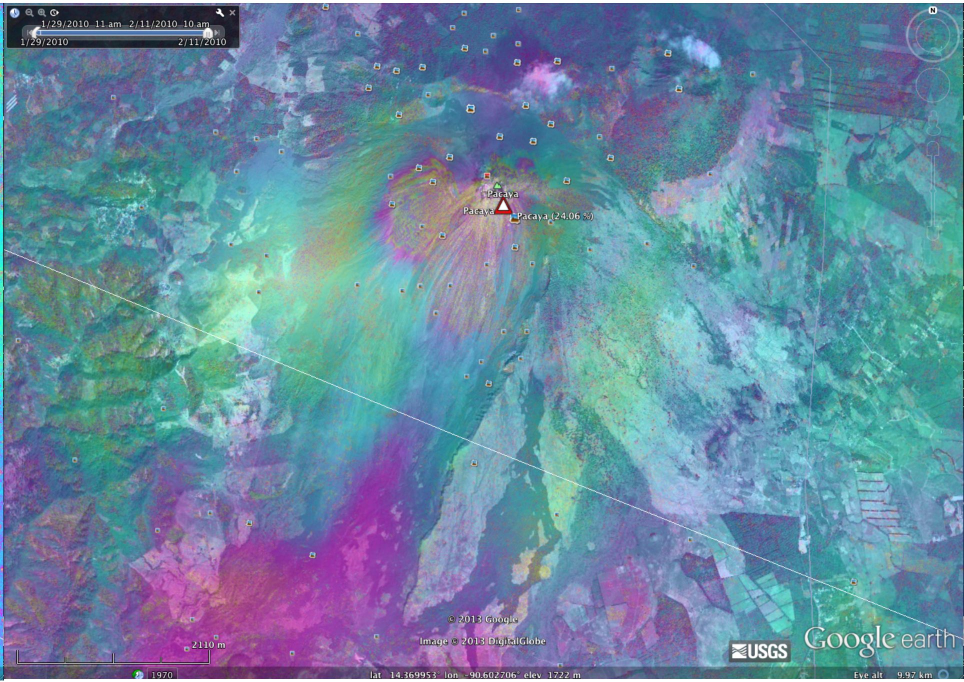

2010/01/29-2010/02/11 UAVSAR interferogram

Proposed Volcano Flight Plans in Japan

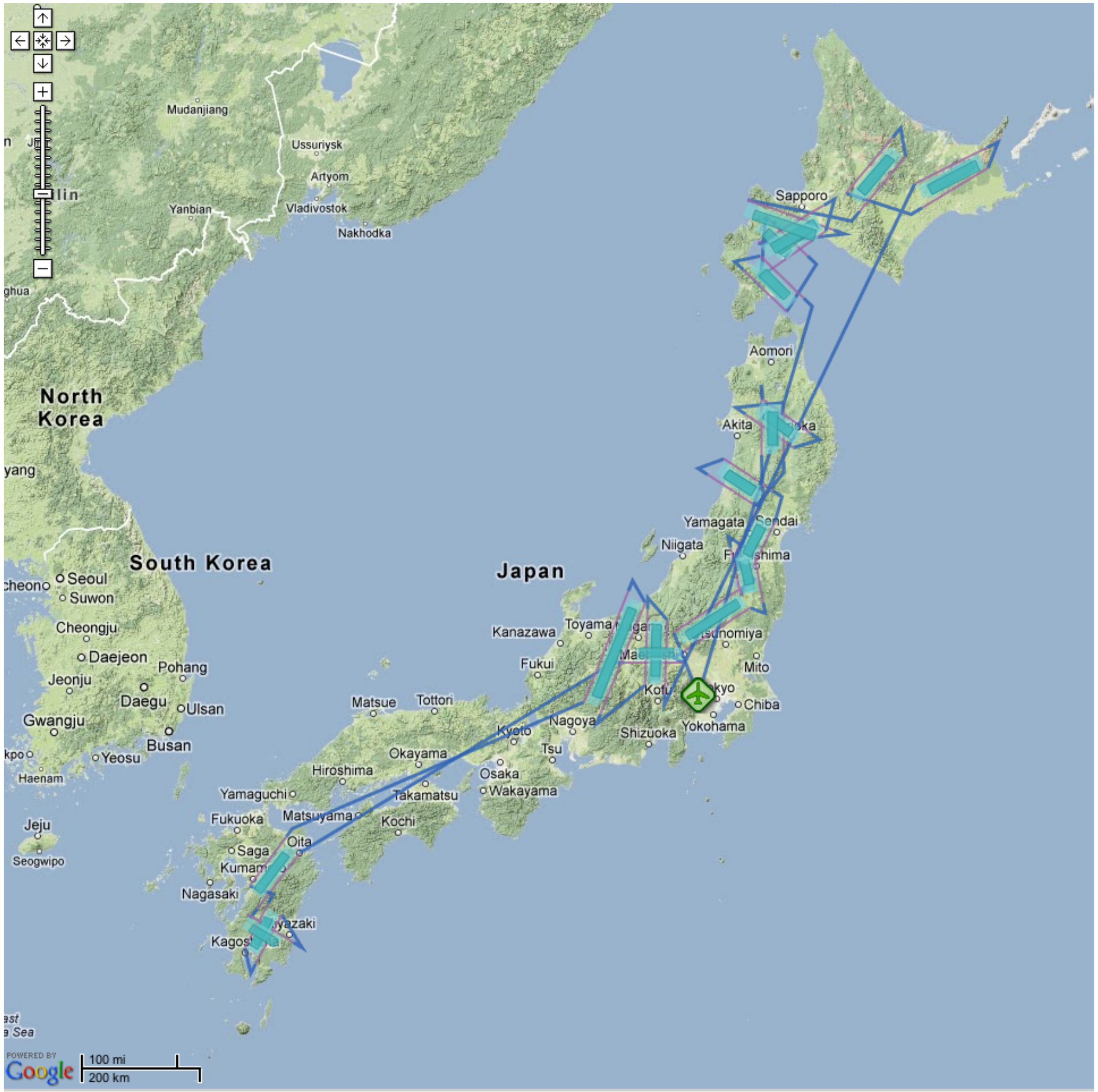

- Volcanoes will be imaged from opposite flight directions in most cases (some will also be flown at 90° for ~3D resolution)
- Repeat interval 1 year
- Possibility to return earlier in case of significant precursory evidence for a future volcano eruption

South America 2013

UAVSAR
Uninhabited Aerial Vehicle Synthetic Aperture Radar

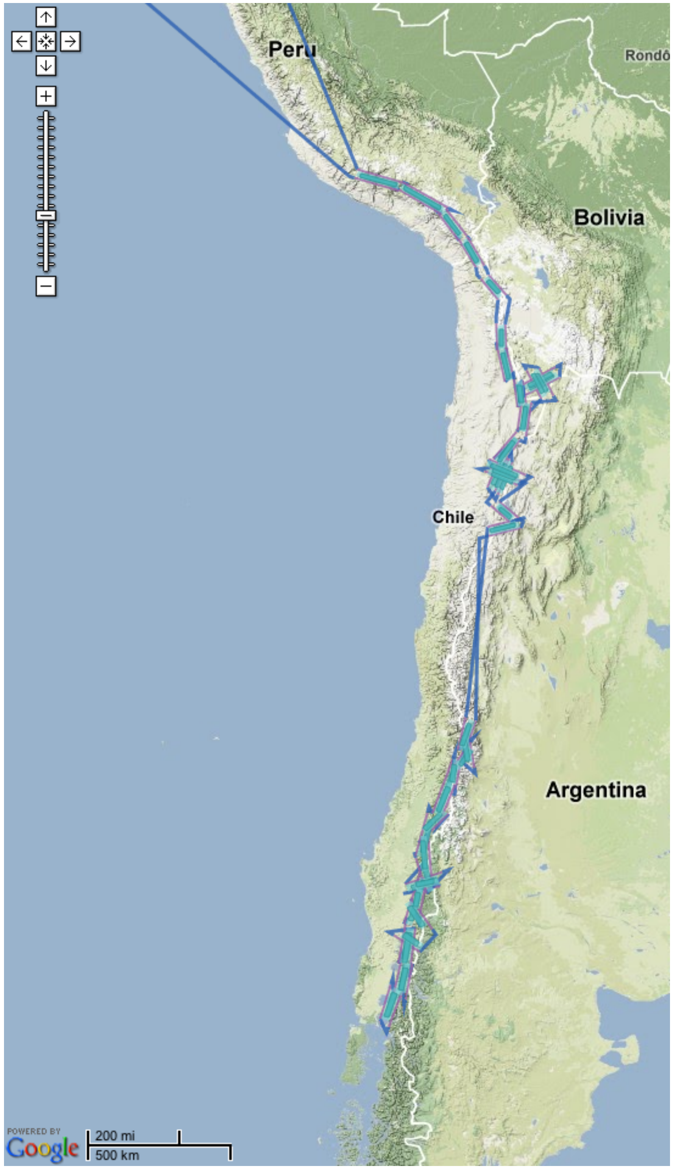

Colombia

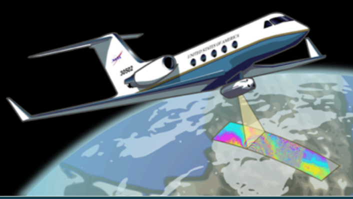

Colombia UAVSAR data from March 2013 flights already processed to polarimetry data products (map on right)

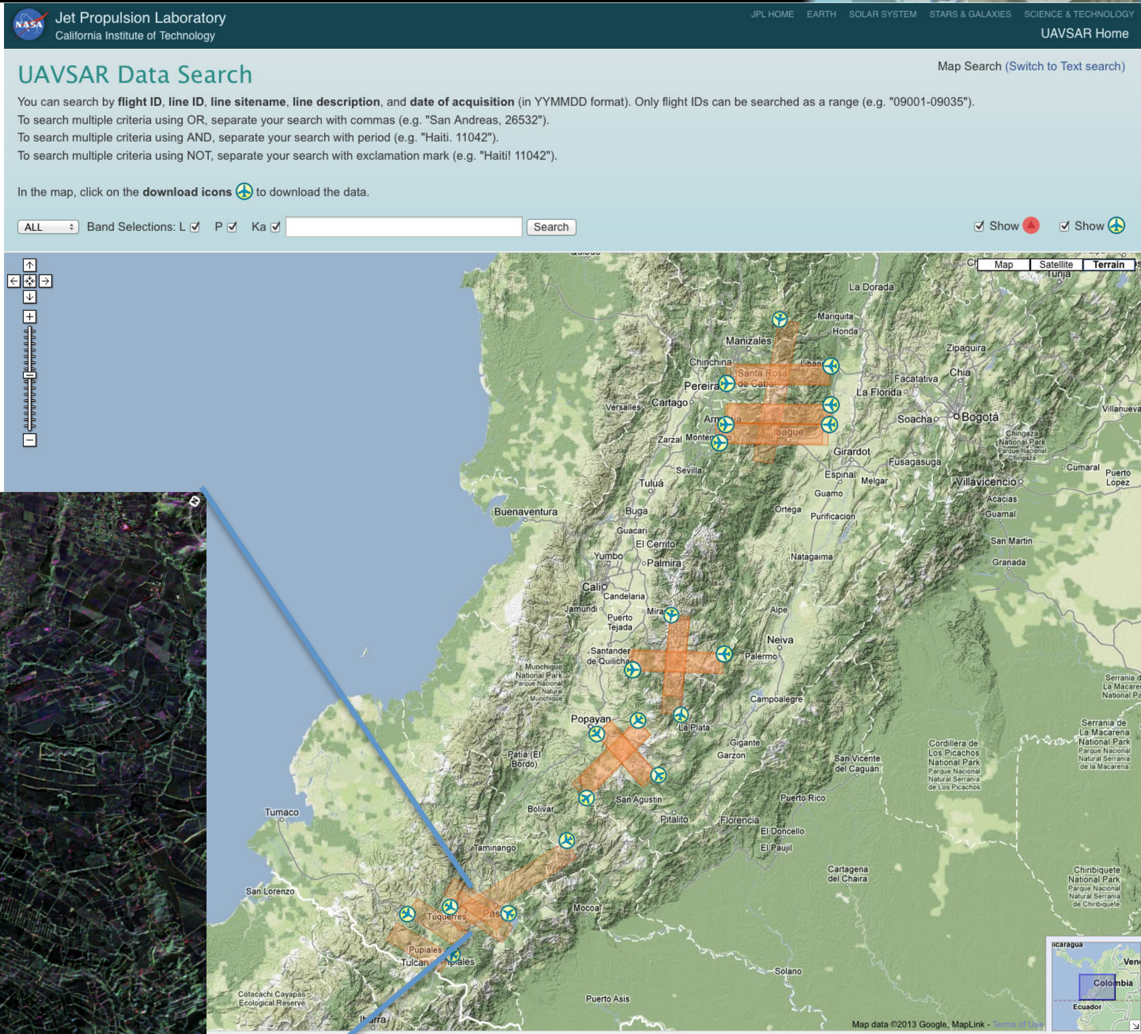

Example over Galeras Volcano

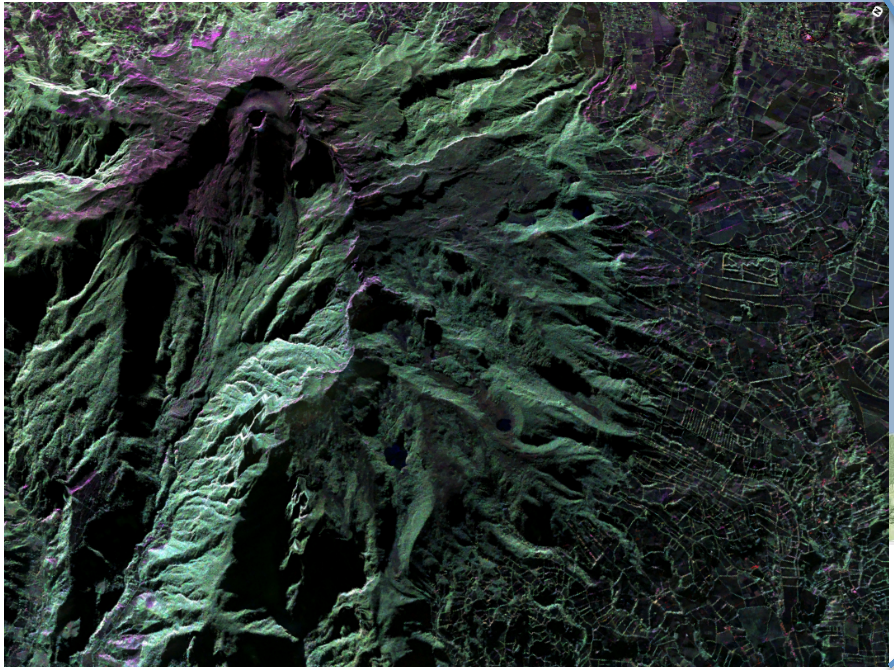

UAVSAR
Uninhabited Aerial Vehicle Synthetic Aperture Radar

Colombia

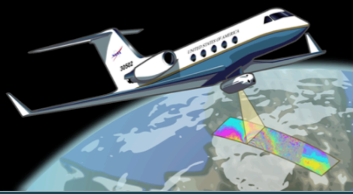

Polarimetry UAVSAR image from Purace volcano

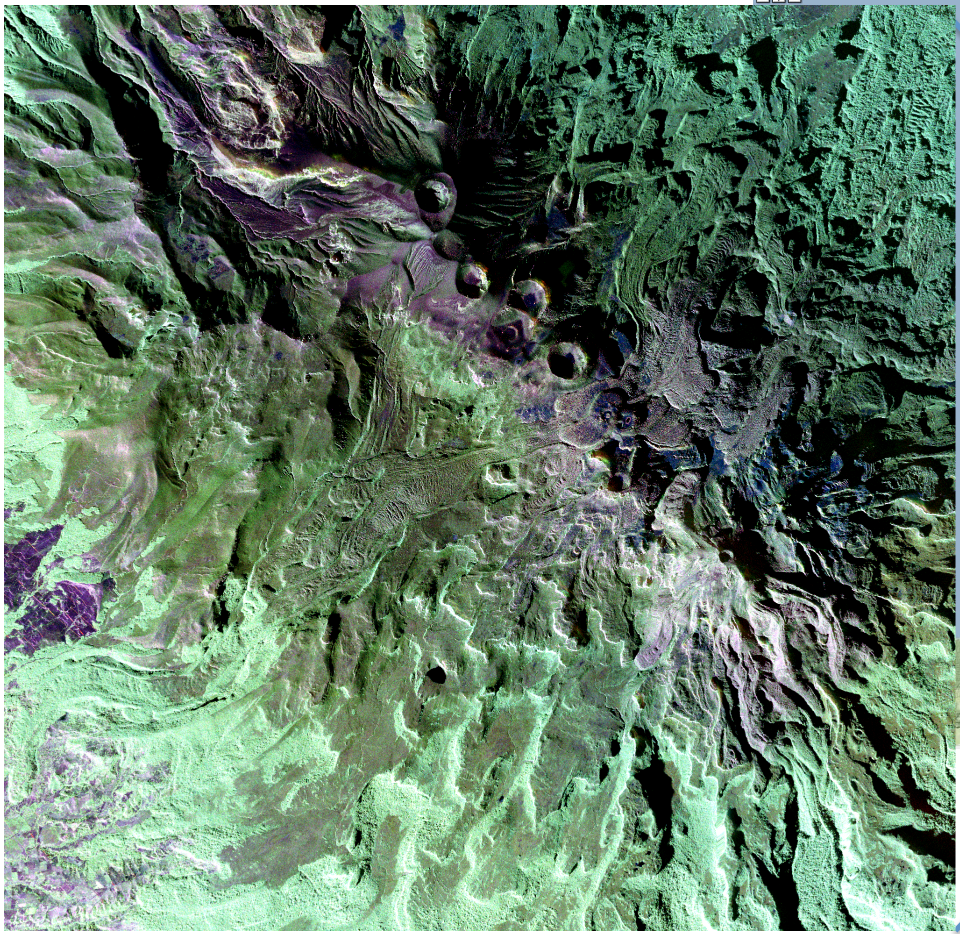

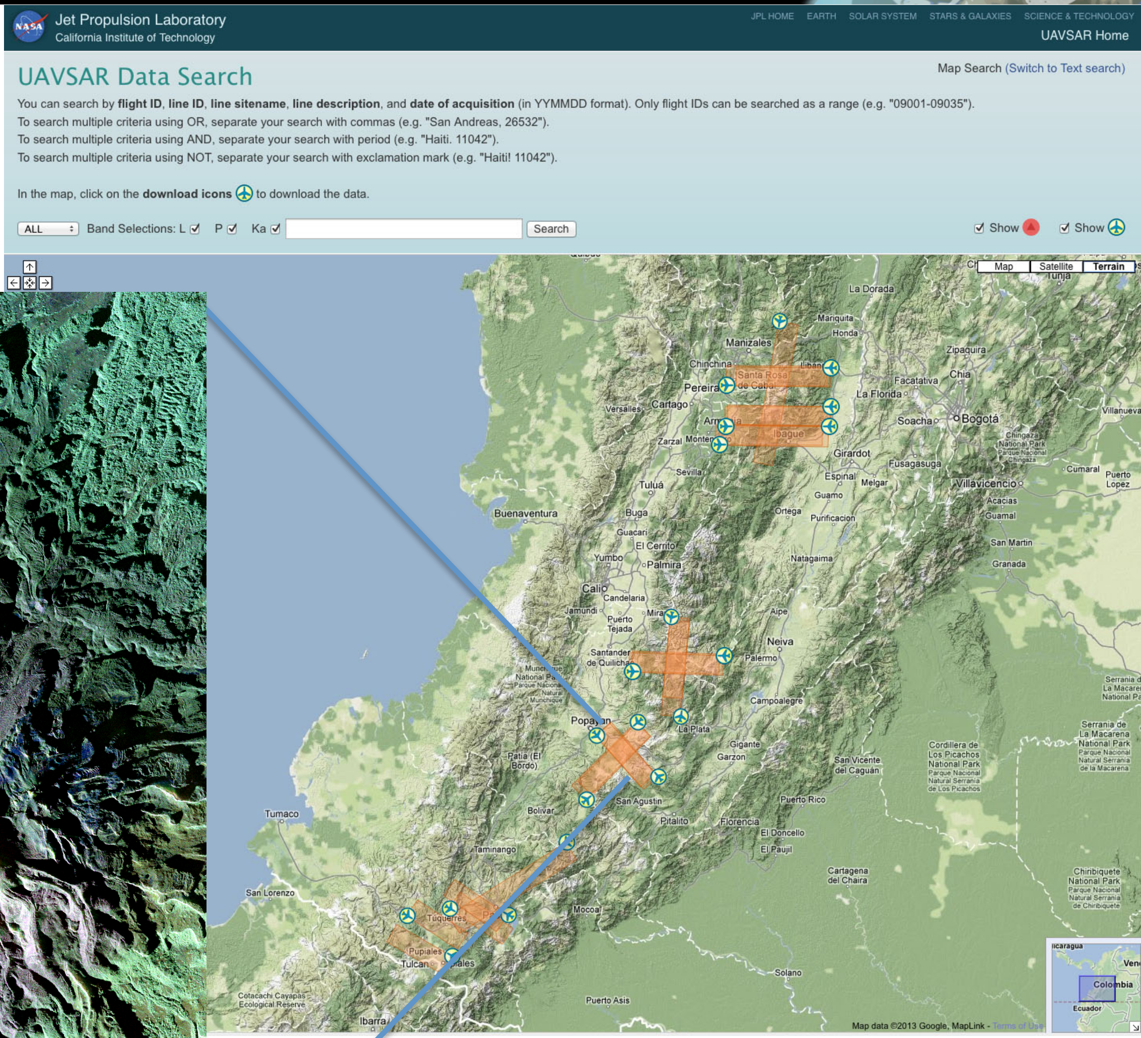

Ecuador

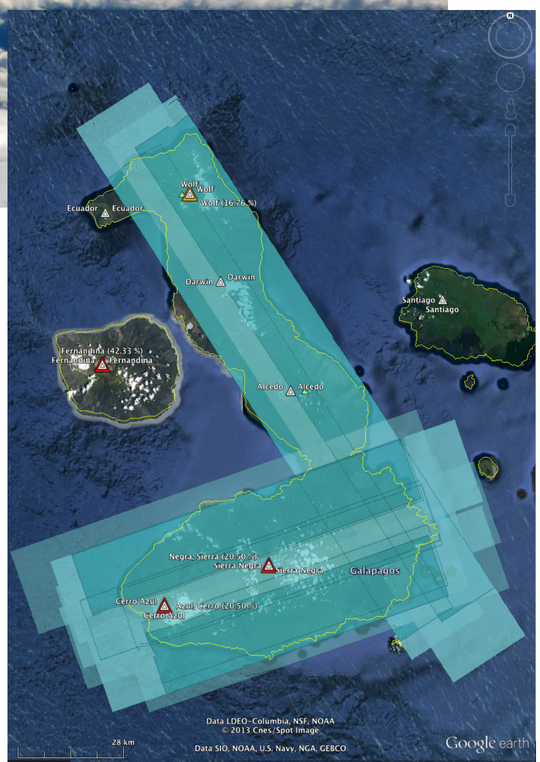
Wolf
Wolf (16.76 %)
Ecuador
Darwin
Santiago
Fernandina (42.33 %)
Fernandina
Alcedo
Negra, Sierra (20.50 %)
Sierra Negra
Galapagos
Cerro Azul
Azul, Cerro (20.50 %)
28 km
Data LDEO-Columbia, NSF, NOAA
© 2013 Cnes/Spot Image
Data SIO, NOAA, U.S. Navy, NGA, GEBCO
Google earth
Tour Guide
lat -0.430184° lon -91.165653° elev 683 m eye alt 117.45 km

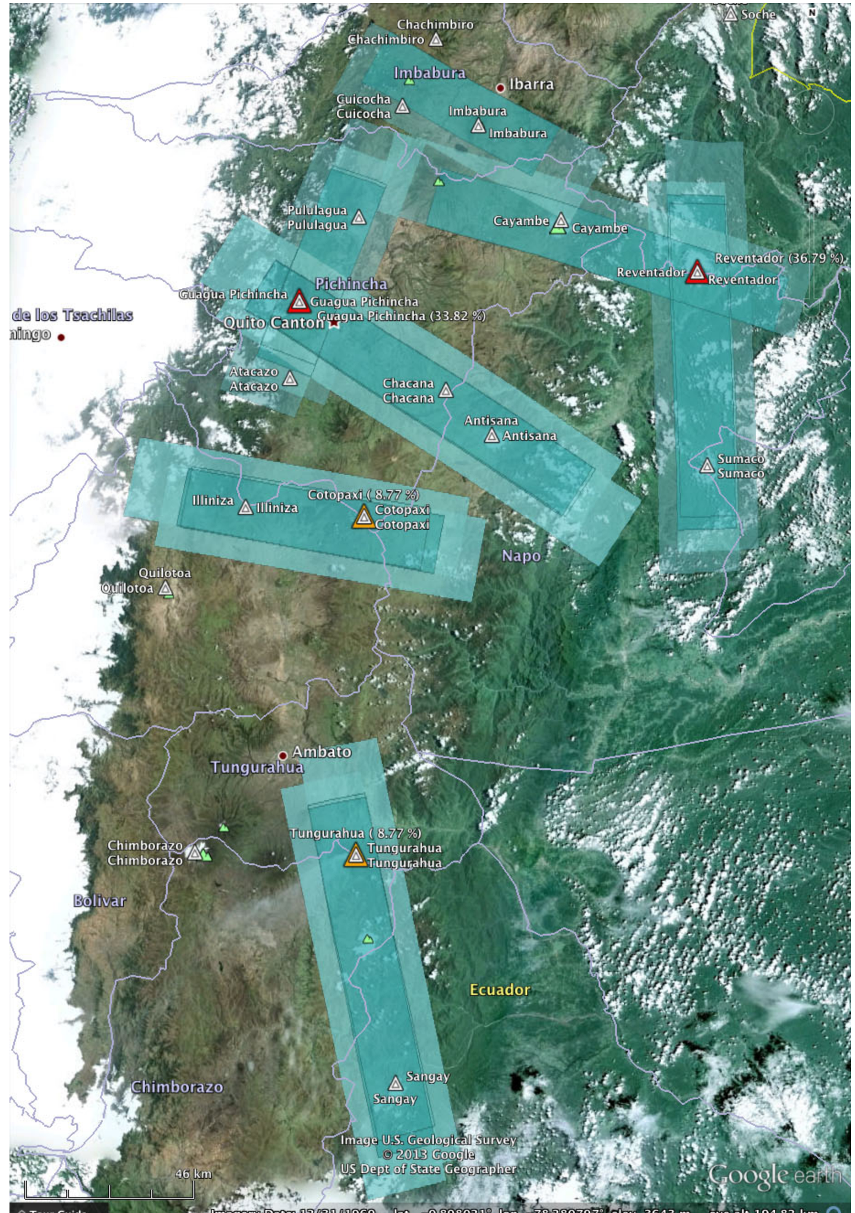
Chachimbiro
Soche
Imbabura
Ibarra
Guicocha
Pululagua
Cayambe
Reventador (36.79 %)
Reventador
Pichincha
Guagua Pichincha
Guagua Pichincha (33.82 %)
Quito Canton
de los Tsachilas
Atacazo
Chacana
Antisana
Sumaco
Illiniza
Cotopaxi (8.77 %)
Cotopaxi
Napo
Quilotoa
Ambato
Tungurahua
Tungurahua (8.77 %)
Chimborazo
Bolivar
Ecuador
Sangay
Image U.S. Geological Survey
© 2013 Google
US Dept of State Geographer
46 km
Google earth
Tour Guide
Imagery Date: 12/31/1969 lat -0.898021° lon -78.280797° elev 3643 m eye alt 194.82 km

Peru

UAVSAR lines flown in 2013: all volcanoes imaged from opposite flight directions

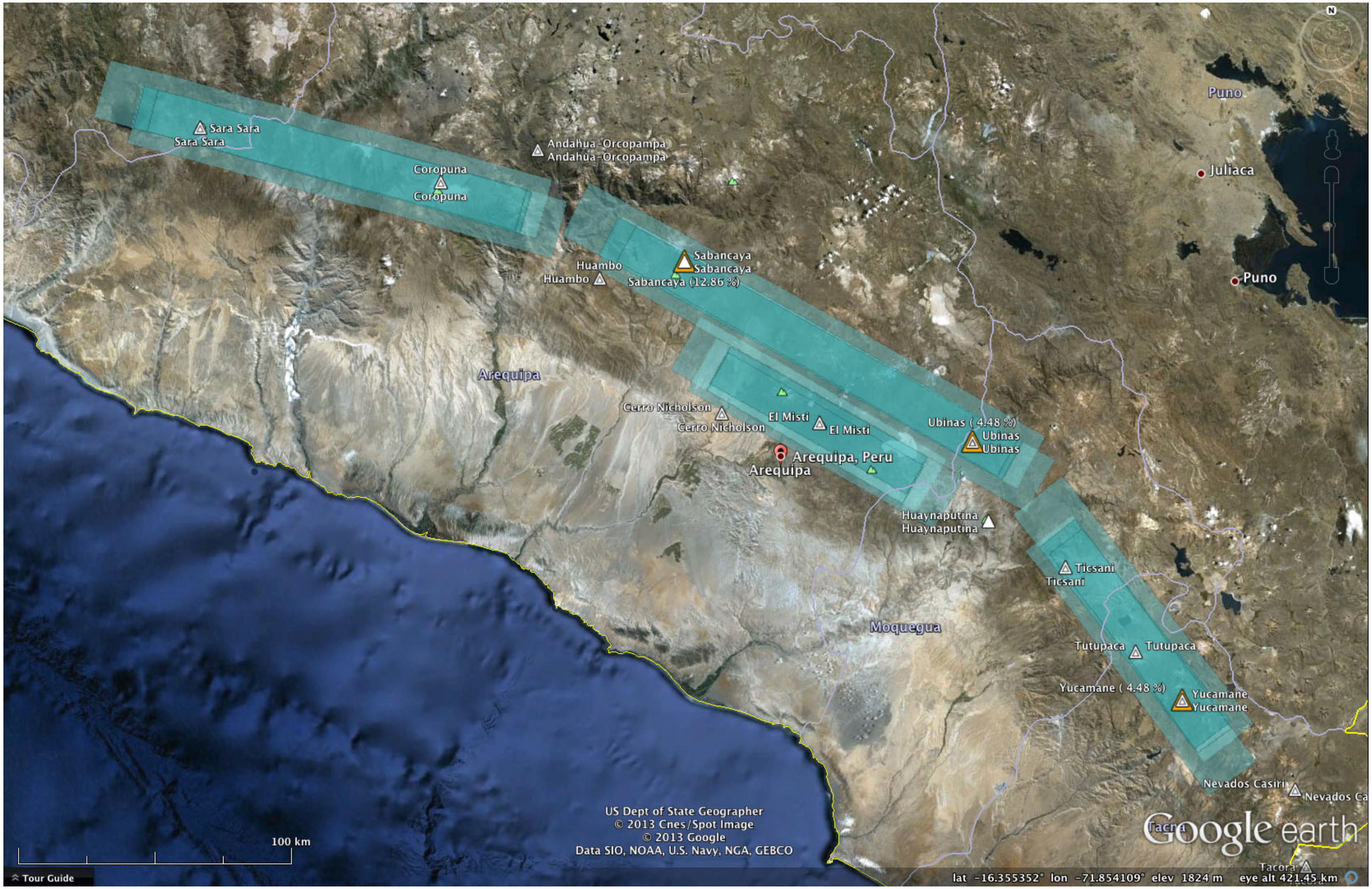

Examples from Kilauea Volcano

Collaborators: M. Poland[2], A. Miklius[2], S.-H. Yun[1], E. Fielding[1], Z. Liu[1], A. Tanaka[3], W. Szeliga[4], S. Hensley[1], and S.Owen[1]

[1]Jet Propulsion Laboratory, California Institute of Technology, Pasadena, CA, USA
[2]Hawaiian Volcano Observatory, U.S. Geological Survey, Hawaiian Volcanoes Nat'l Park, HI, USA
[3]Geological Survey of Japan, AIST, Tsukuba, Ibaraki, Japan
[4]Dept. of Geological Sciences, Central Washington University, Ellensburg, WA, USA

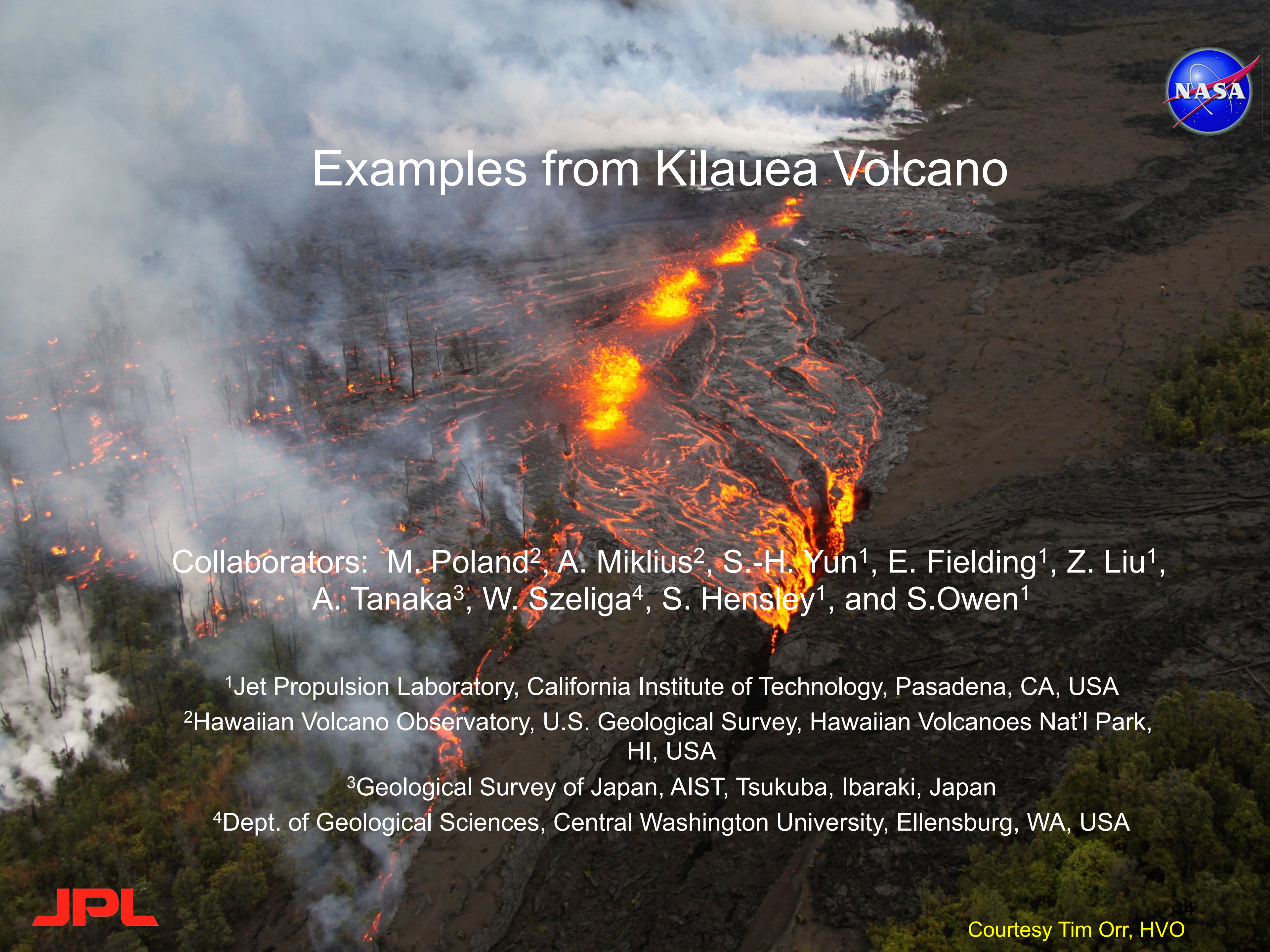

Courtesy Tim Orr, HVO

Kilauea, Hawaii

UAVSAR
Uninhabited Aerial Vehicle Synthetic Aperture Radar

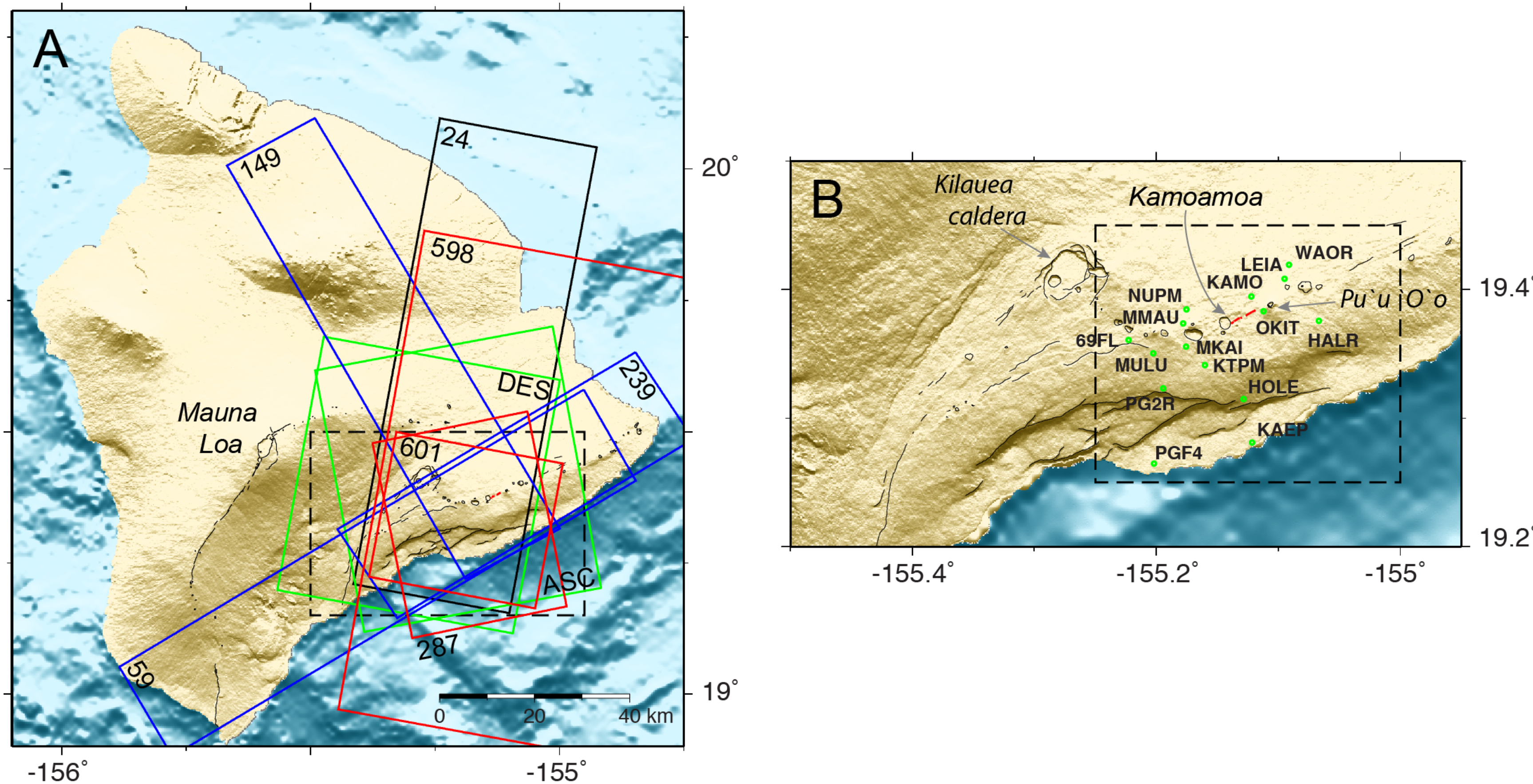

Hawaii InSAR tracks (A) and (B) Kilauea/E Rift focus area around Kamoamoa eruption (fissures in red, courtesy T. Orr, HVO, GPS sites green dots)

DI Events: January 2010

Kilauea Caldera Deflation-Inflation events

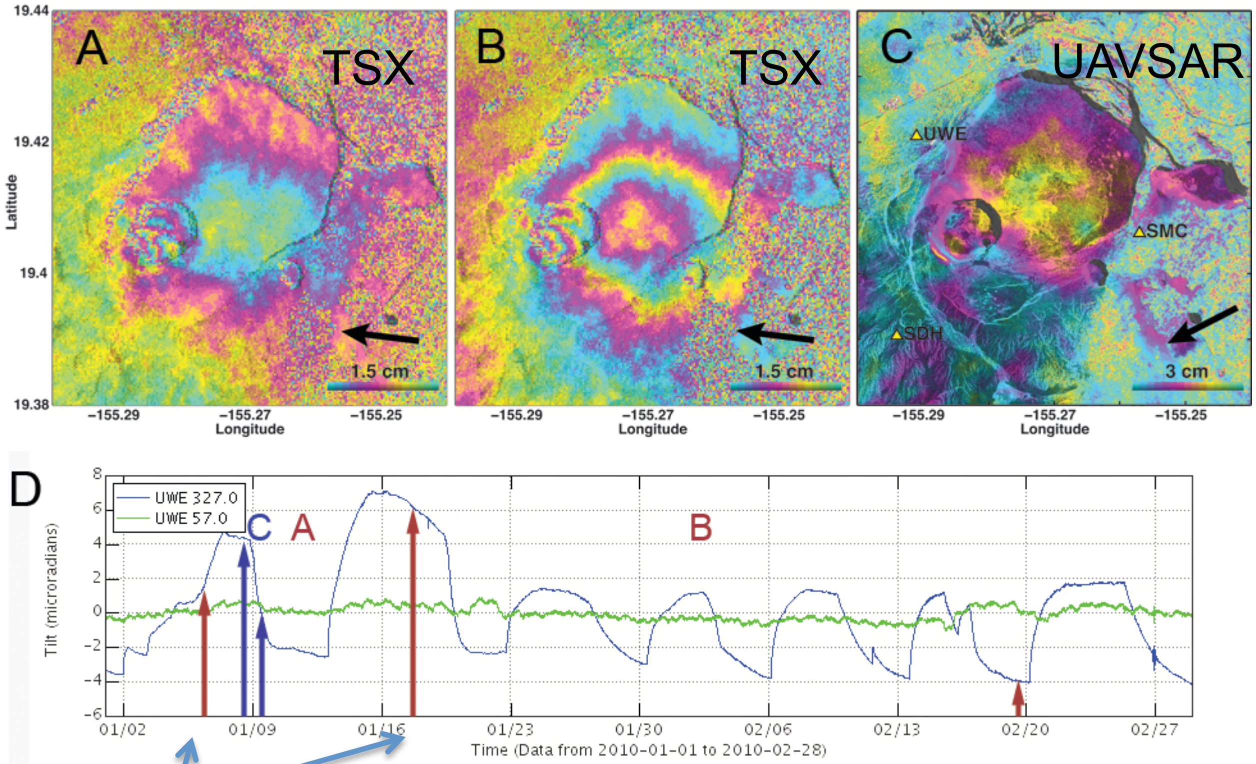

UWE electronic tilt meter

SAR acquisitions

March 5-9, 2011 Kamoamoa Eruption

Kilauea summit tilt

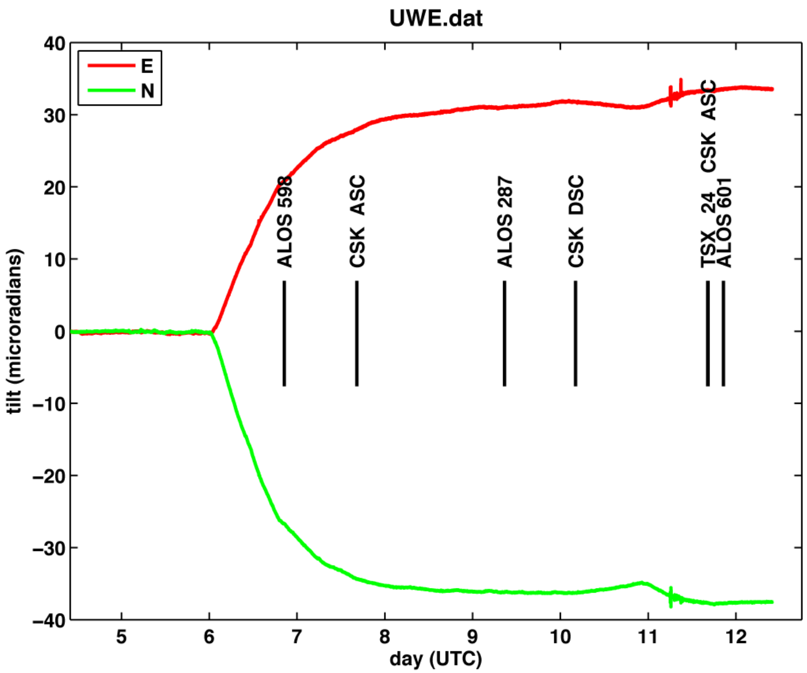

ERZ Fissure eruption

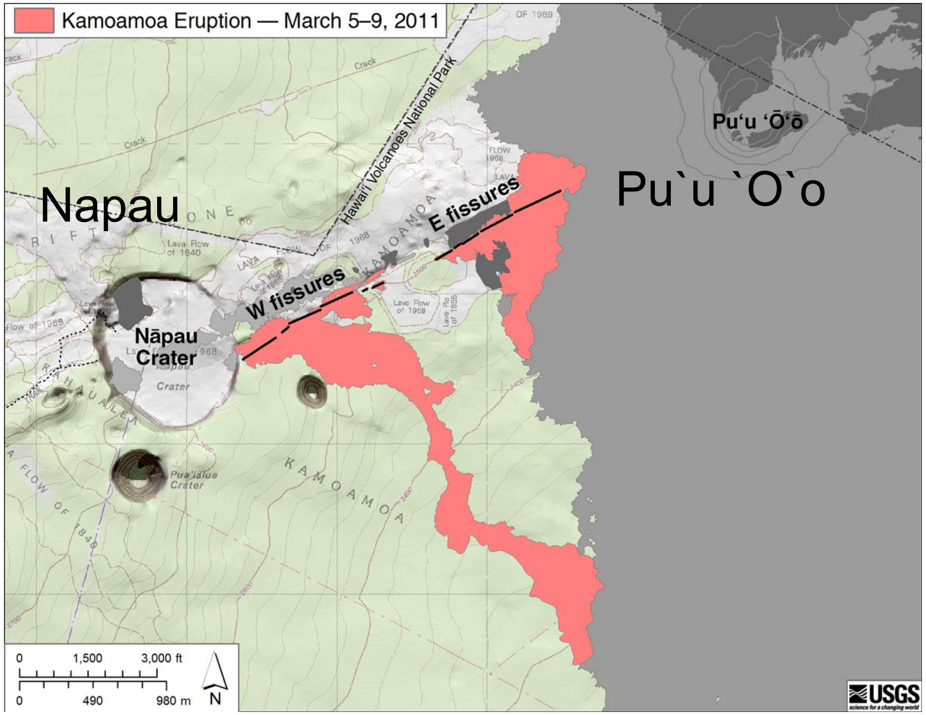

Eruption started late afternoon March 5 (HST) with Pu`u `O`o tilt (deflation) starting 30 min prior to Kilauea tilt (deflation)

Near-real time COSMO-SkyMed data

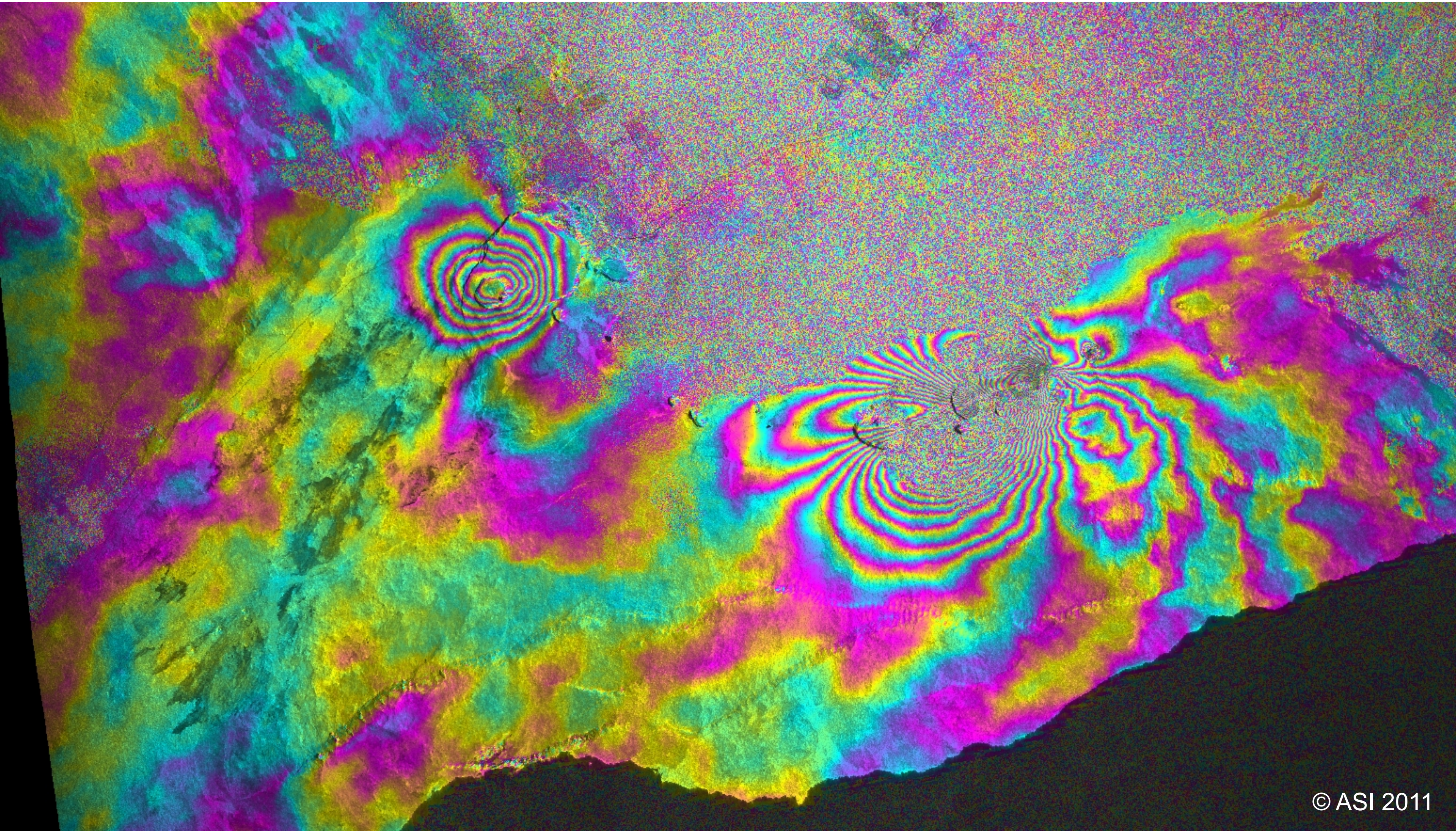

1st interferogram on March 7, ~12 hrs after acquisition

UAVSAR spanning eruption

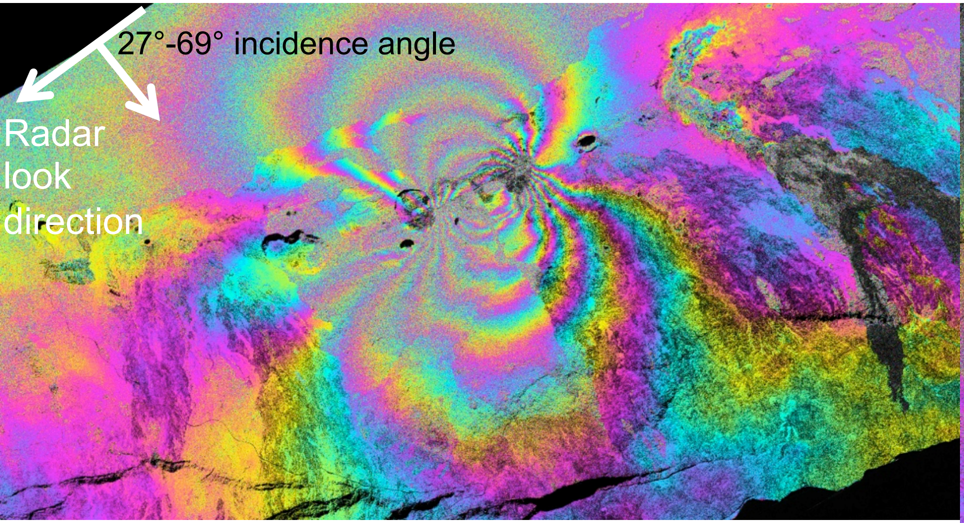

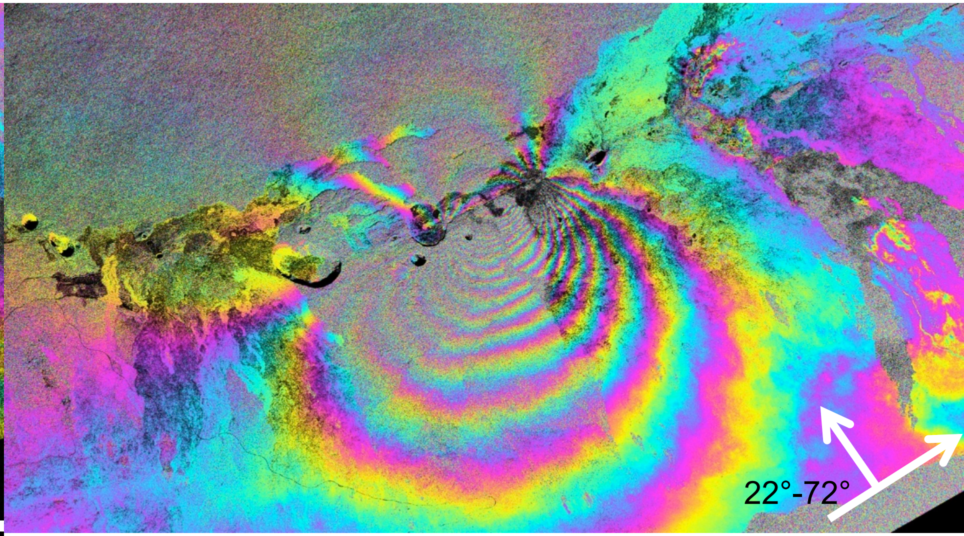

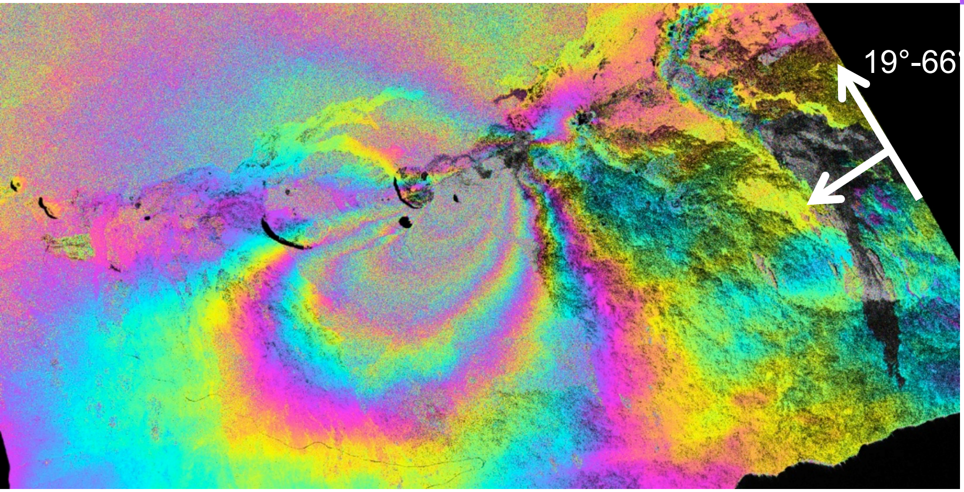

UAVSAR interferograms, (Jan 2010 – May 2011), 1.4 years, spanning the March 5-9, 2011 eruption

uavsar.jpl.nasa.gov for more info.

The March 2011 Kilauea Fissure Eruption

UAVSAR
Uninhabited Aerial Vehicle Synthetic Aperture Radar

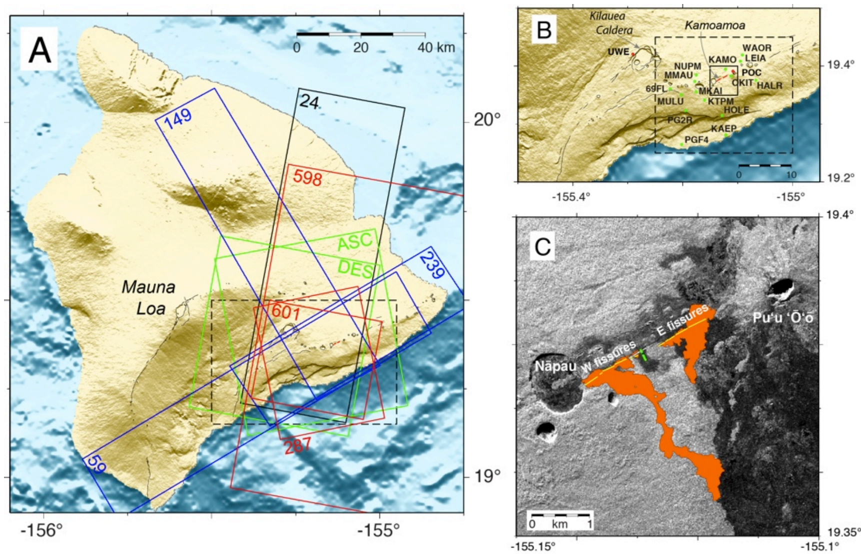

UAVSAR plus satellite InSAR and GPS data were used to constrain the detailed dike opening models and dike volume history shown in the next slide.

Figure 1. Maps of Hawaii, Kīlauea Volcano, and the Kamoamoa eruption area. (A) Satellite and airborne SAR processed scenes: in red, ALOS tracks, green, COSMO-SkyMed, black, TerraSAR-X, and blue, UAVSAR. (B) Close-up view of Kilauea, showing GPS sites (green dots), tilt meter sites (red dots), and the Kamoamoa fissures (red lines). Dashed box shows the interferogram area and the smaller solid box is the area shown in (C). (C) Close-up view of the fissures and lava flows.

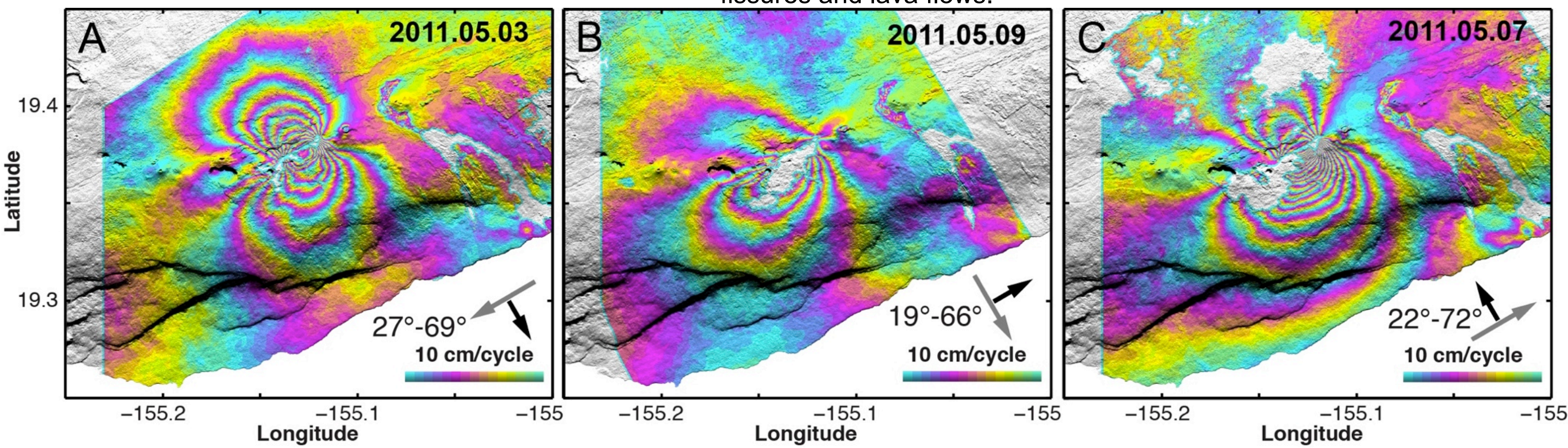

Figure 2. UAVSAR interferograms for the dashed box area in Fig. 1B. Each interferogram is from a different viewing directions as indicated by the aircraft heading (gray) and look direction (black) arrows and their near to far range ground incidence angles.

UAVSAR
Uninhabited Aerial Vehicle Synthetic Aperture Radar

Interferograms ending March 6-11

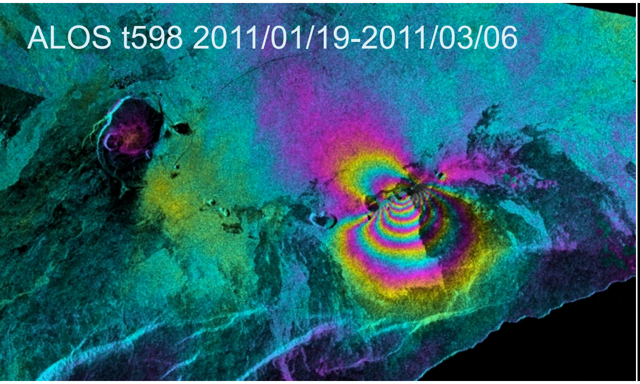

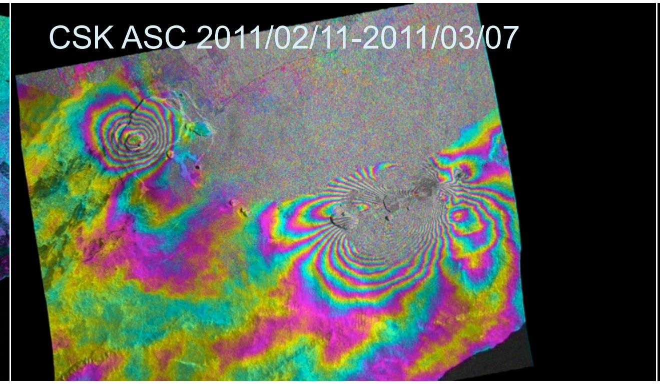

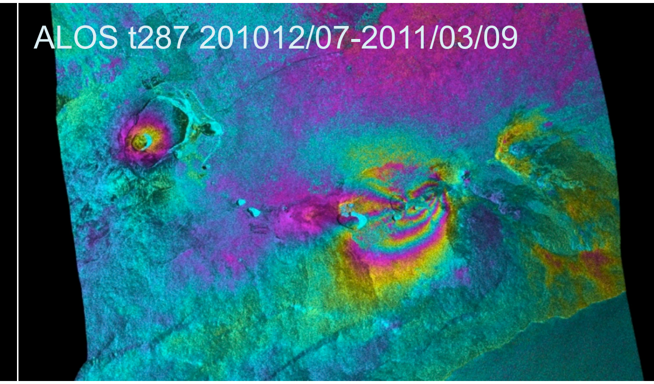

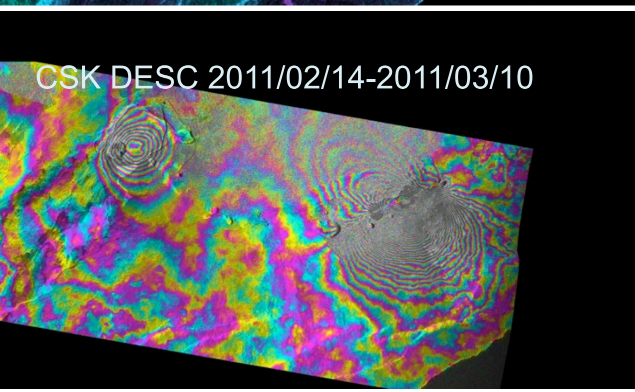

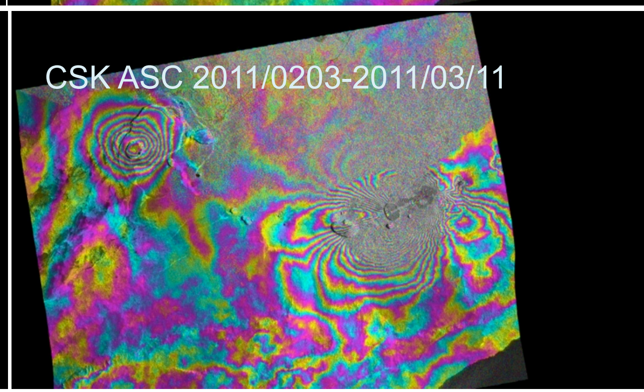

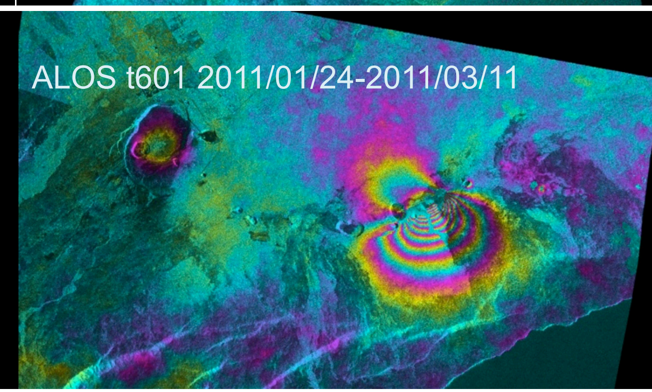

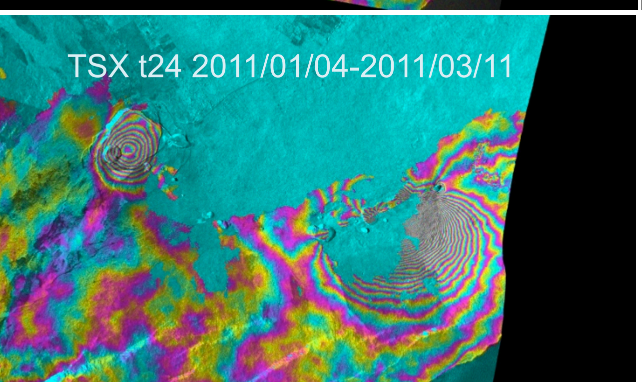

L-band (ALOS) better coherence vs X-band
(but higher noise over bare rock)

Unwrapped interferograms: 12 cm/cycle ALOS; 1.5 cm/cycle TSX and CSK

The March 2011 Kilauea Fissure Eruption

UAVSAR
Uninhabited Aerial Vehicle Synthetic Aperture Radar

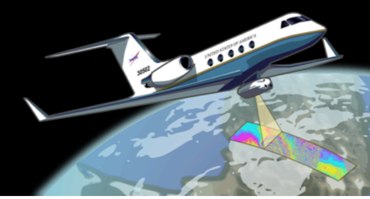

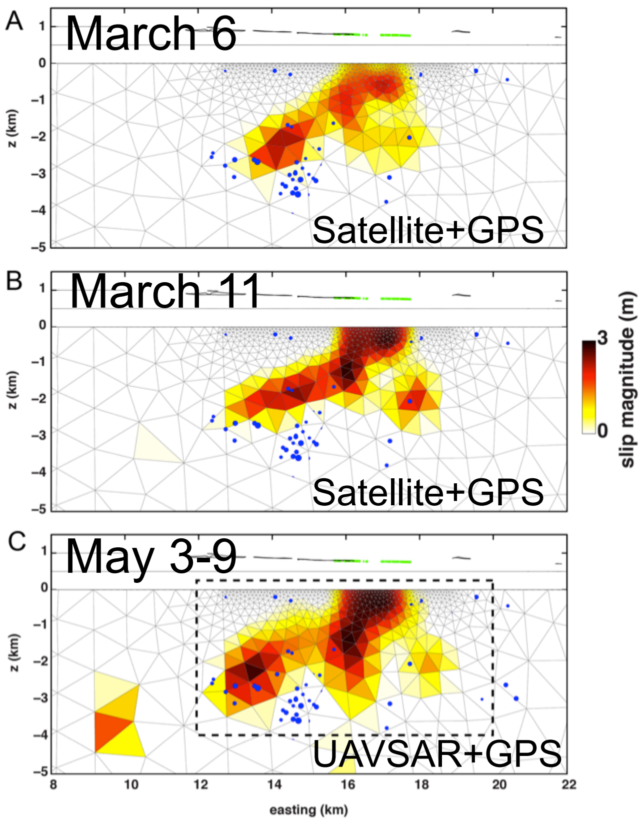

Figure 3. InSAR + GPS constrained model side views of dike opening for three dates: March 6, within 24 hours of the eruption start (ALOS); March 11, after the end of the eruption (ALOS, CSK, TSX); and early May (UAVSAR). The models show growth in amount of opening and area and suggest the dike was fed from its deeper limb plunging to the left and a shallower limb to the right.

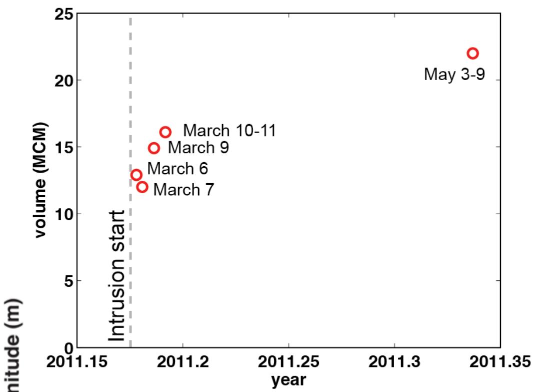

Figure 4. Dike volume increase as a function of time for the dates with InSAR data and models. Following the end of the eruption (March 9) there was continued dike volume increase as shown by the March 10-11 model and the UAVSAR constrained May models.

Dike models give a detailed view of the dike complexity and details that help explain the simultaneous feeding of the dike from sources beneath both Kīlauea Caldera and Puʻu ʻŌʻō.

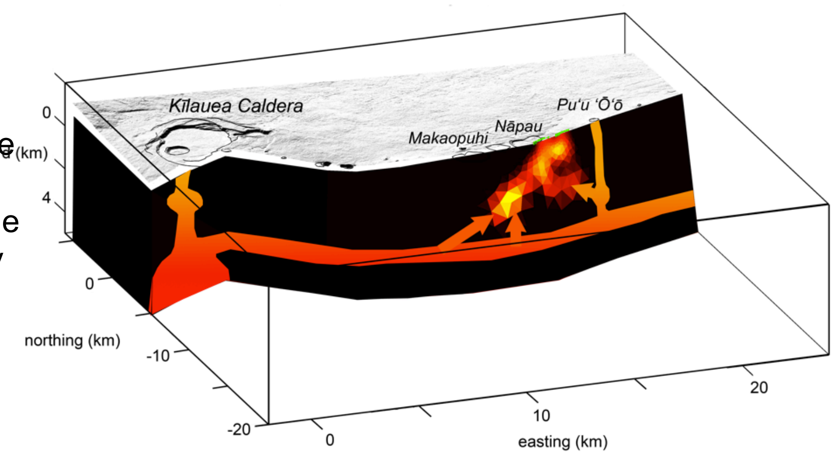

Figure 5. Conceptual model for the Kīlauea magmatic system related to the summit caldera source, the Puʻu ʻŌʻō conduit, and the ERZ conduit thought to exist below 3 km depth. Model for March 6 is shown, red arrows show our interpretation of magma feeding the dike intrusion from the ERZ conduit from the up-rift limb of the dike and from the Puʻu ʻŌʻō conduit in the down-rift direction.

Post-diking deformation…

UAVSAR
Uninhabited Aerial Vehicle Synthetic Aperture Radar

InSAR time series 2010.5 – 2012.2

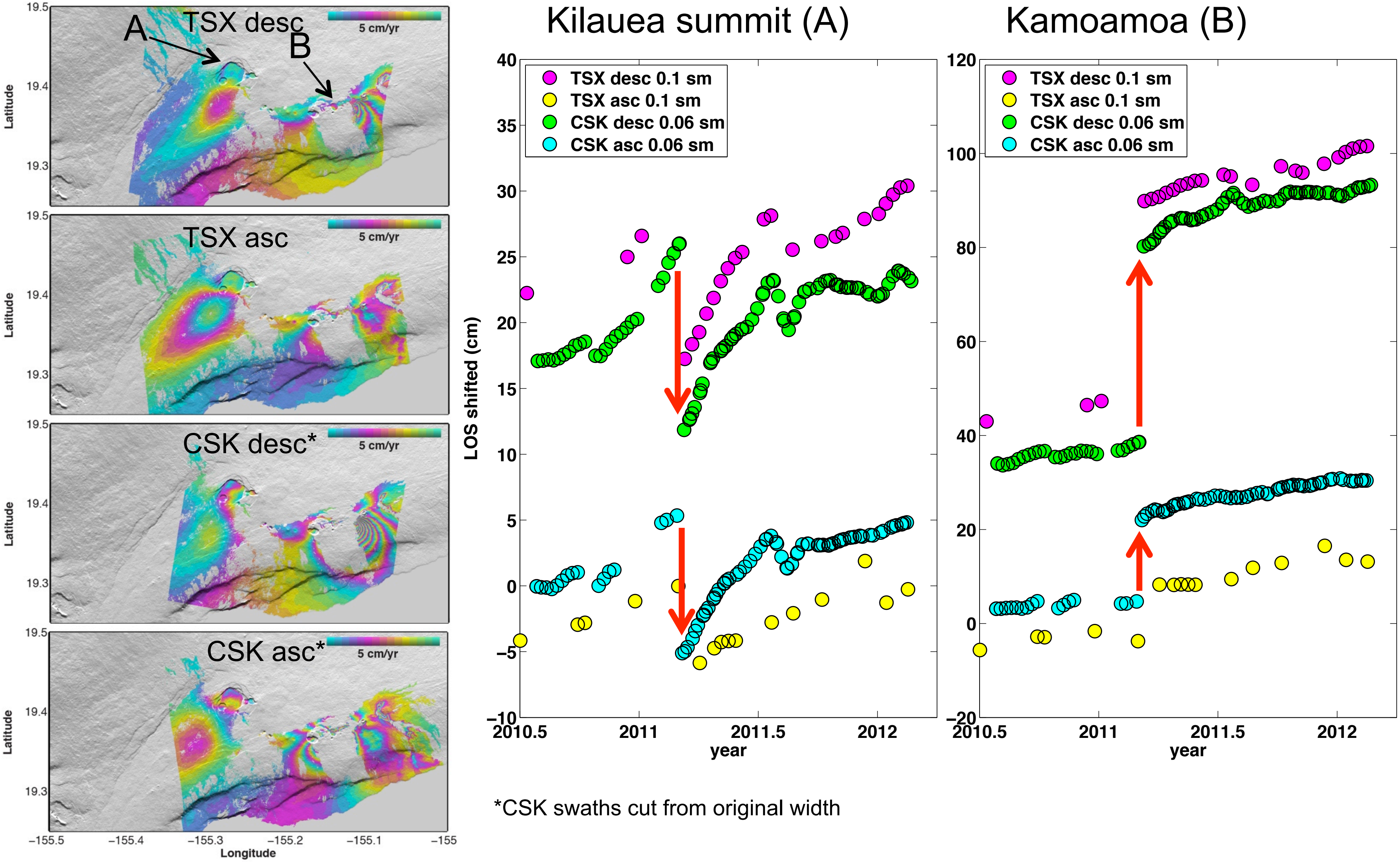

*CSK swaths cut from original width

Post-diking deformation from InSAR time series

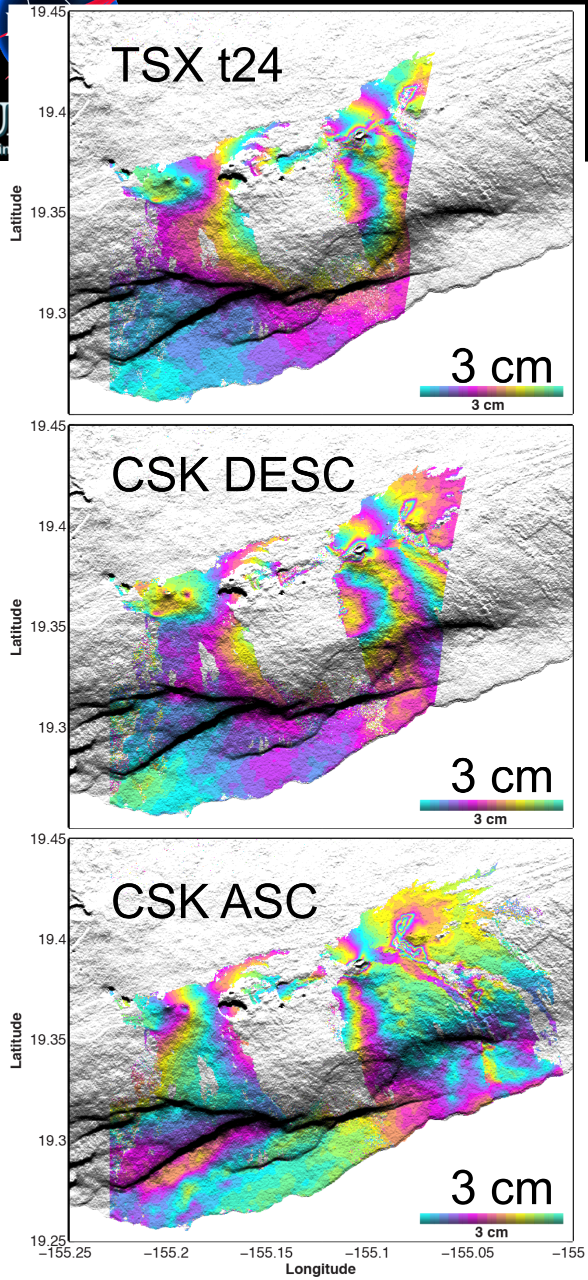

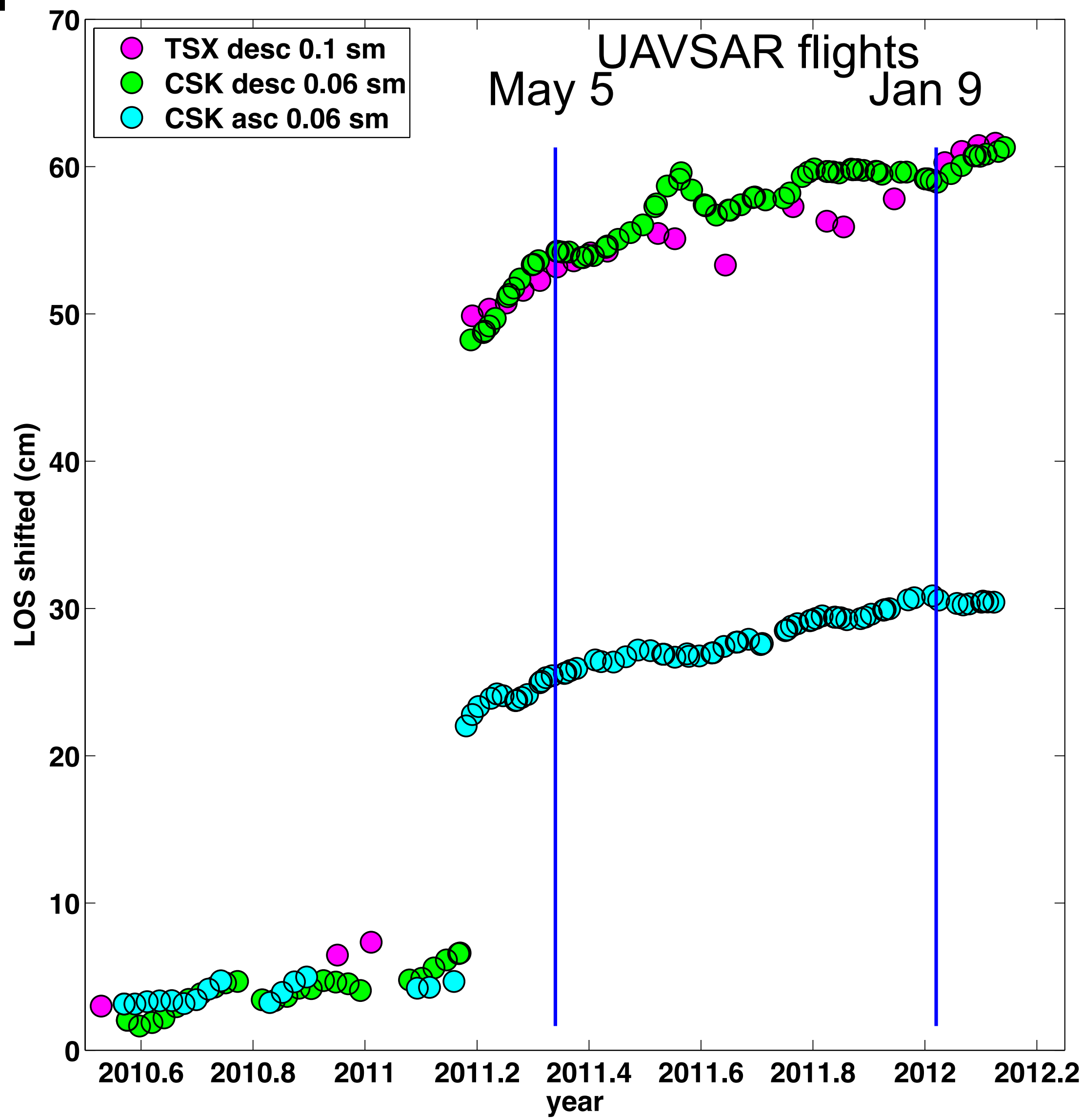

displacements

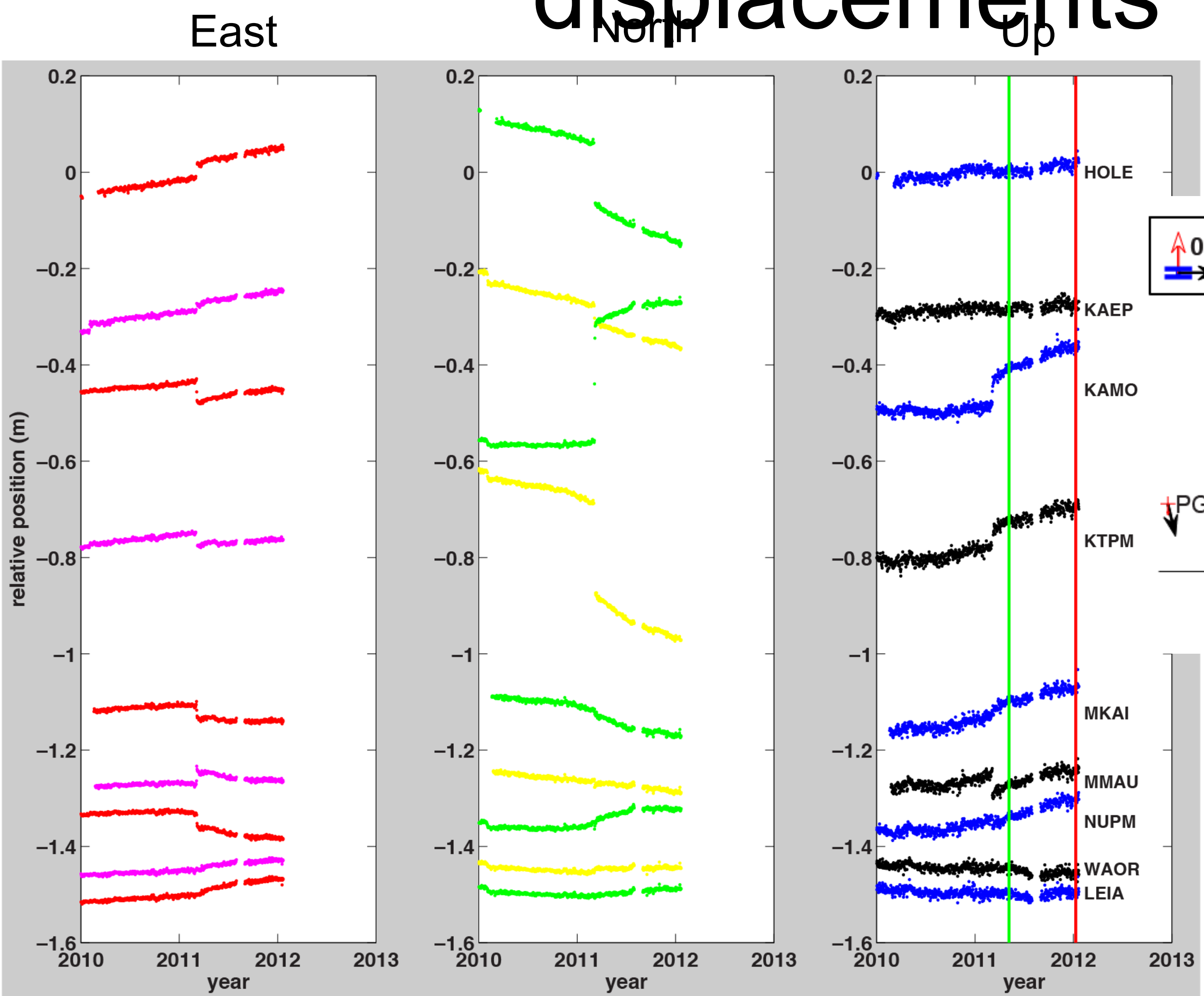

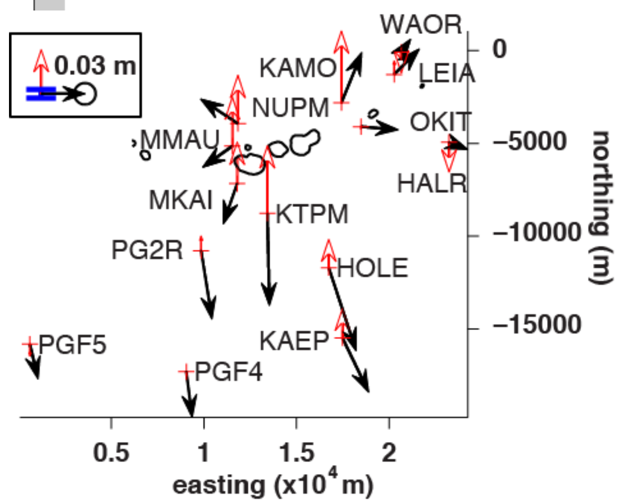

UAVSAR flight dates shown by green/red lines through U time series. TS shown for only a subset of GPS sites on map.

UAVSAR post-diking: line 239

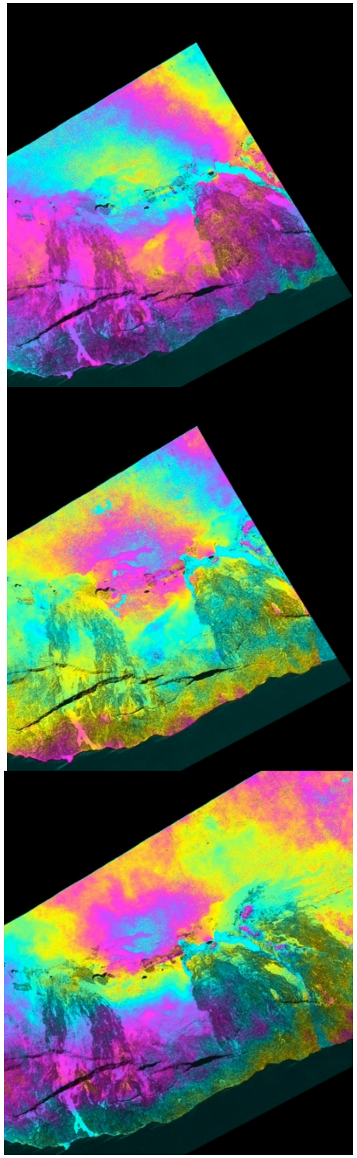

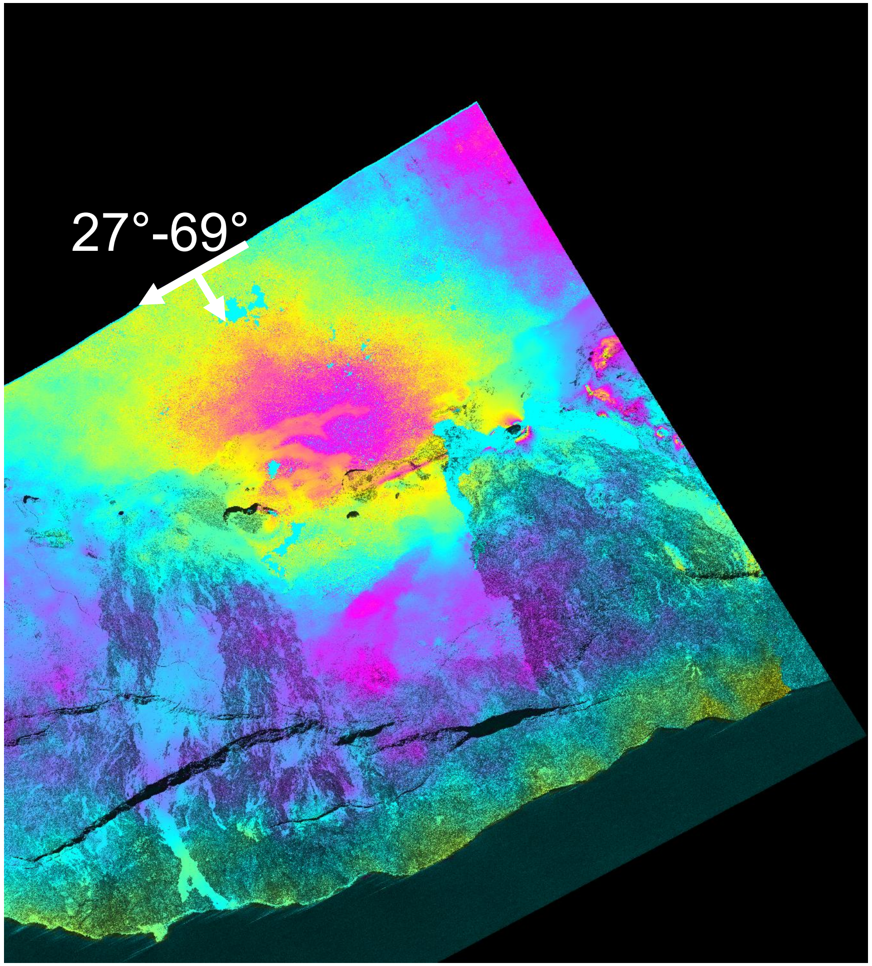

(*right*) Three independent interferograms. (*left*) stack of the three interferpgrams

UAVSAR post-diking: line 59

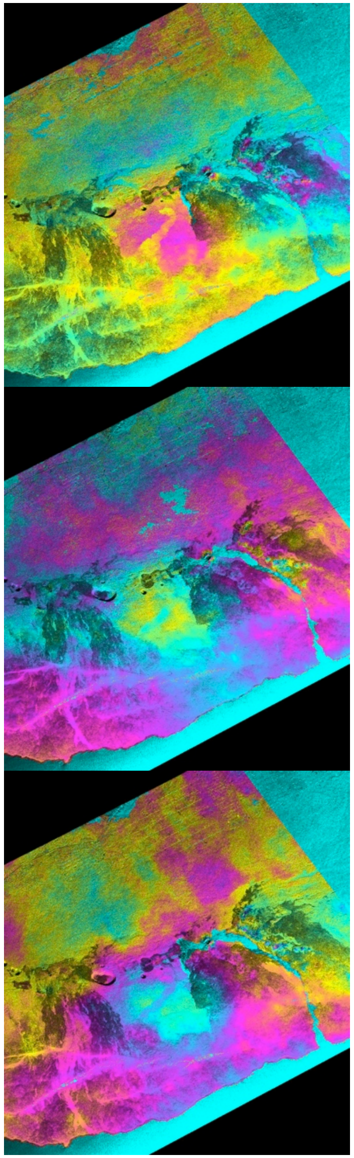

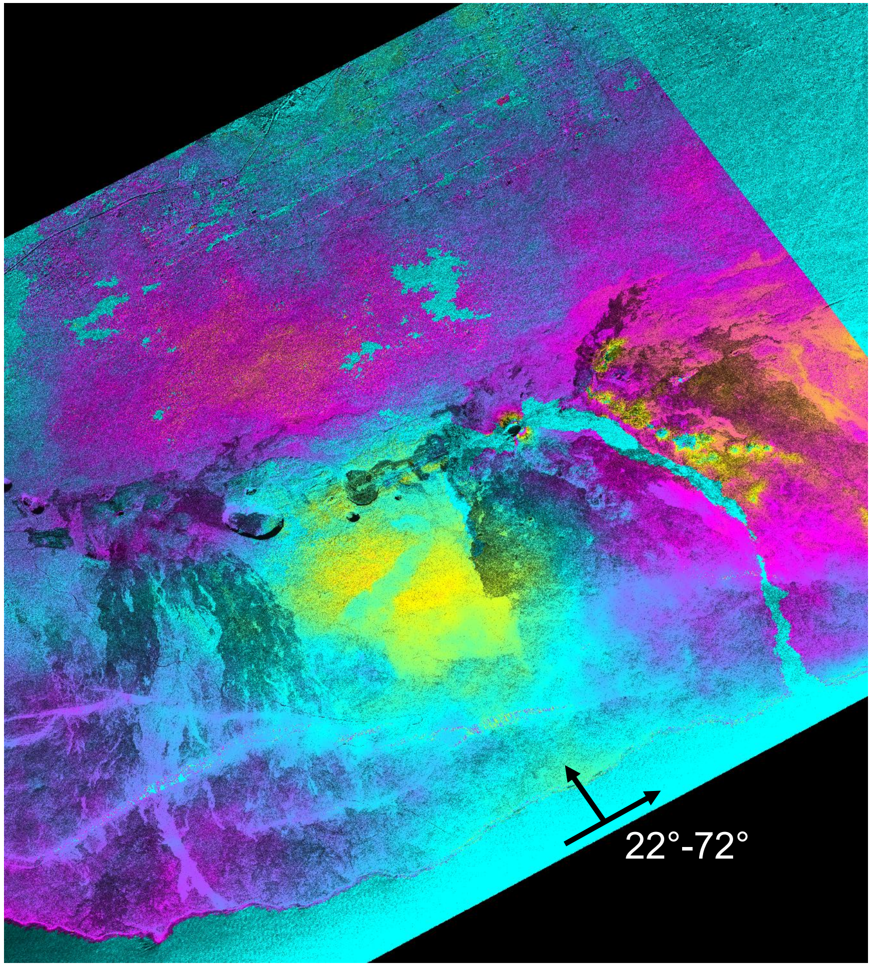

(*right*) Three independent interferograms.
(*left*) stack of the three interferograms

Post-diking MCMC modeling

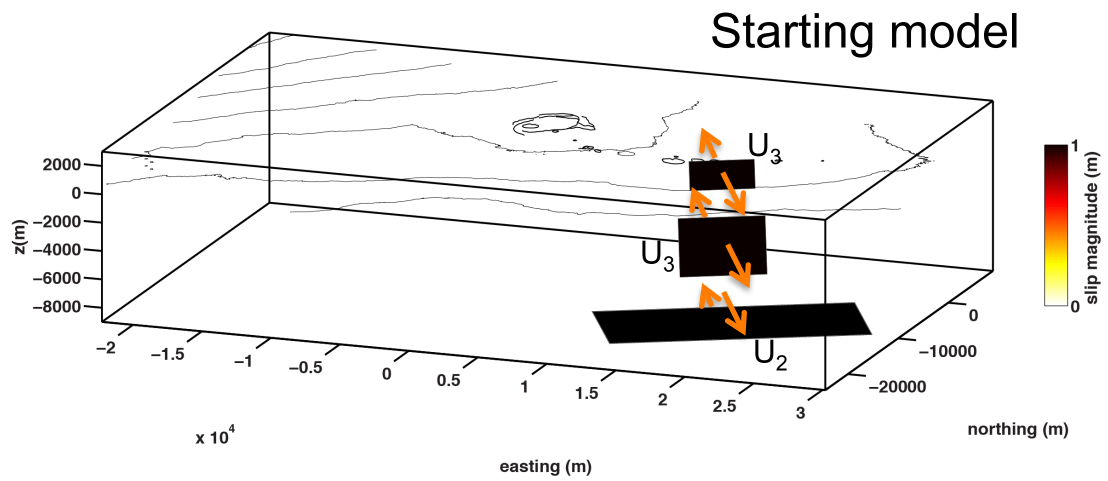

Model set-up was designed to address the type of process observed by Desmarais and Segall (2007):

- near vertical dikes in starting model
- horizontal detachment fault

Post-diking TSX, CSK,

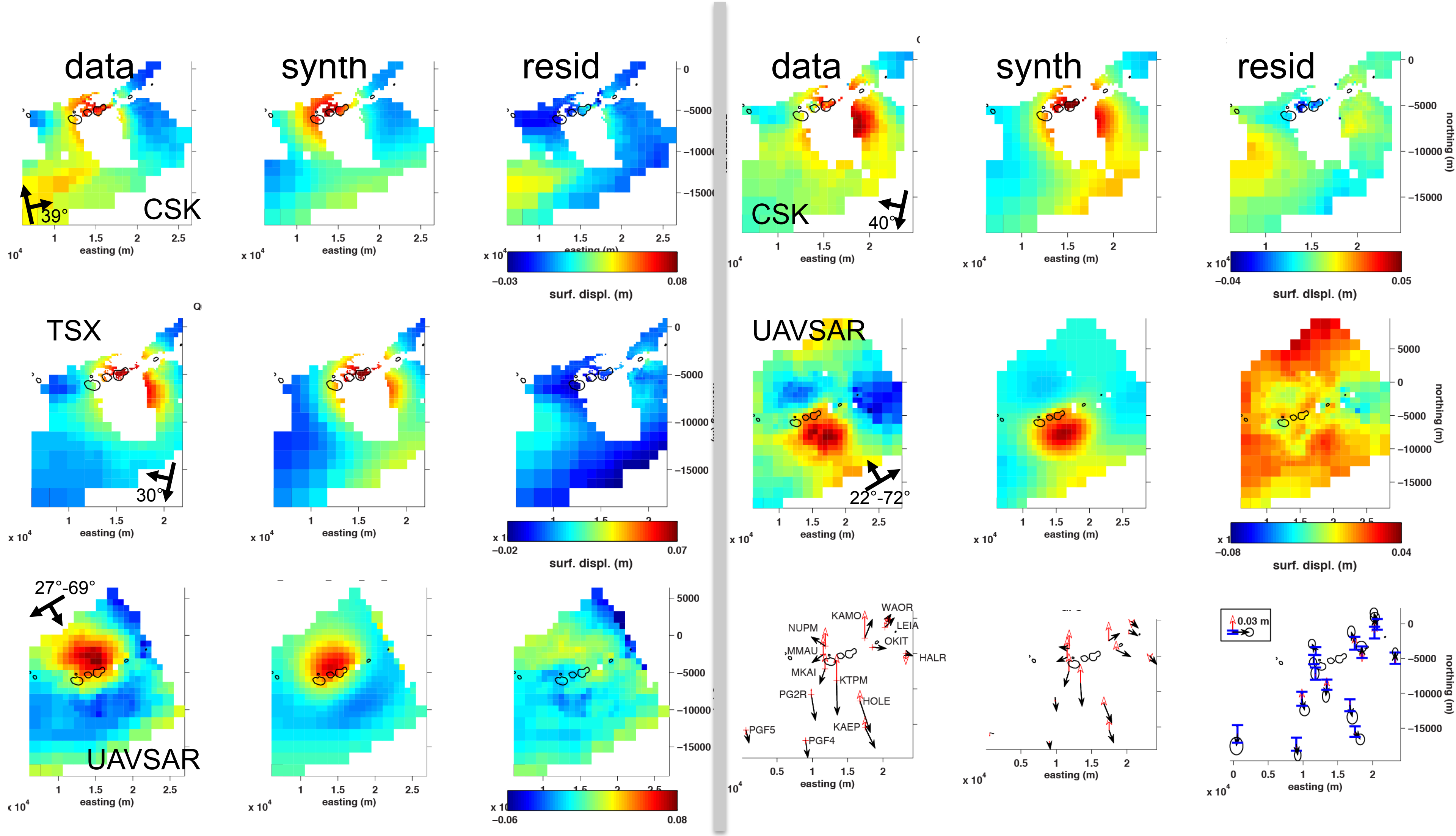

Post-diking MCMC modeling

Starting model

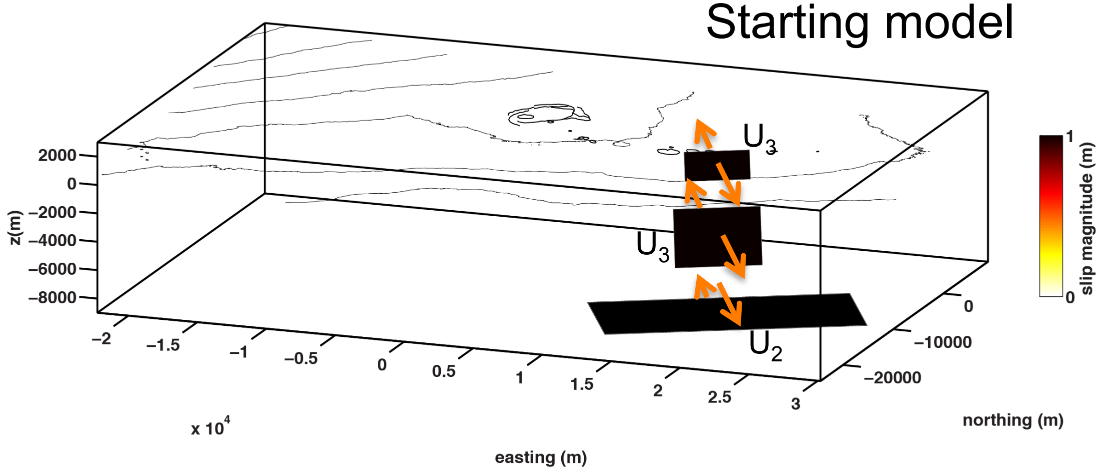

MCMC model after 10^6 iterations

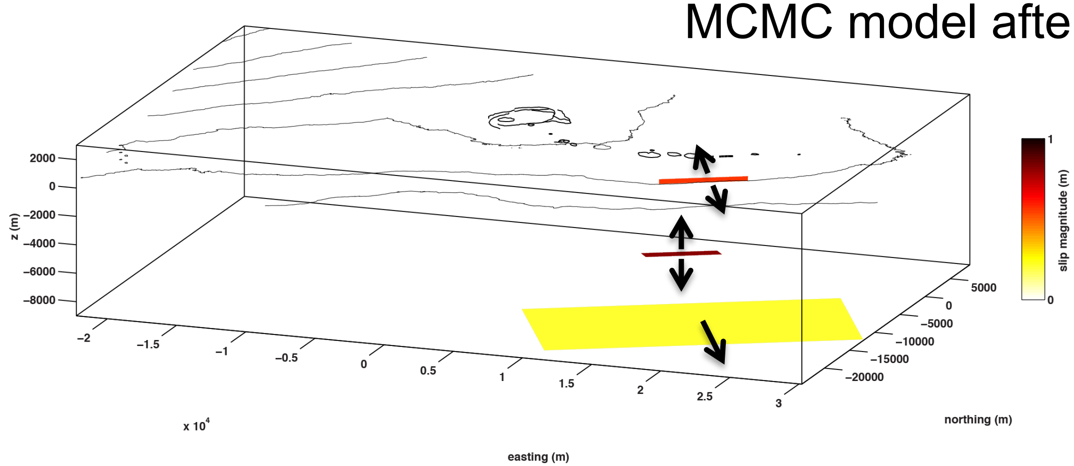

Co-eruption $\Delta\sigma$ viewed from W

Sill opening promoted

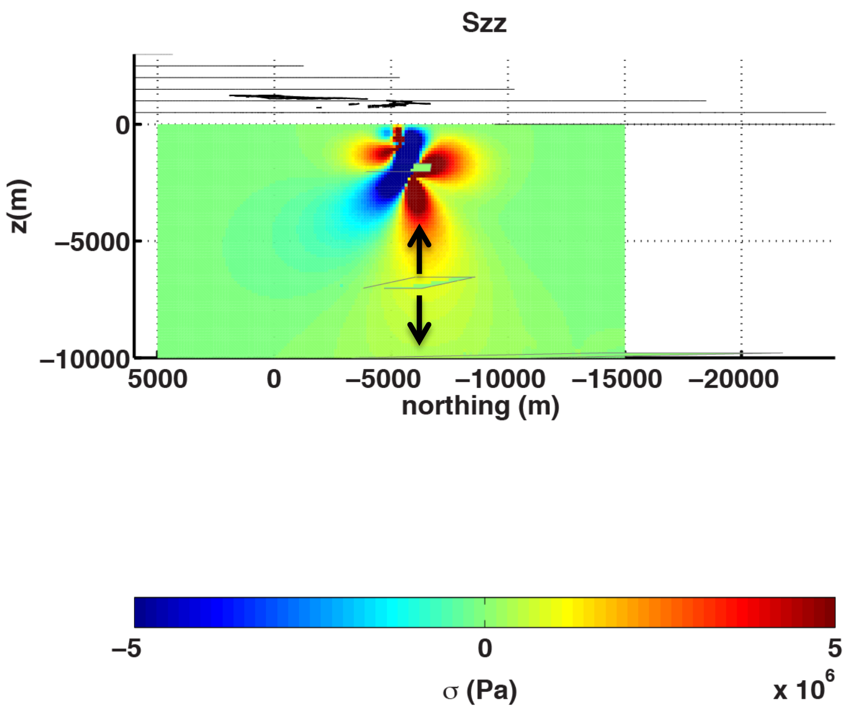

Positive Szz promotes opening of horizontal sills

Shallow dike opening inhibited, but in area of complex stress change

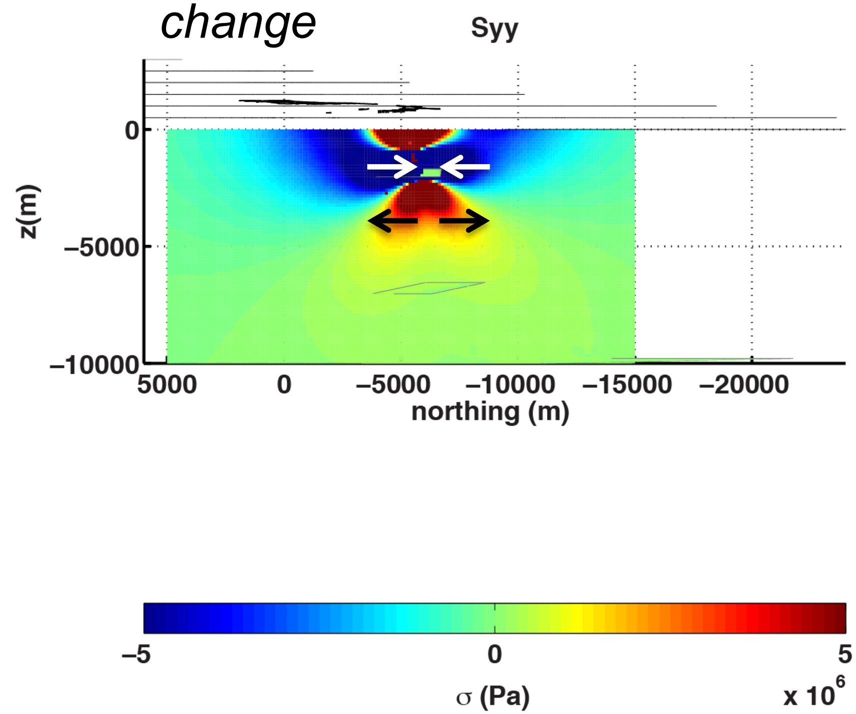

Positive Syy promotes opening of vertical dikes

Comparison with past dikes

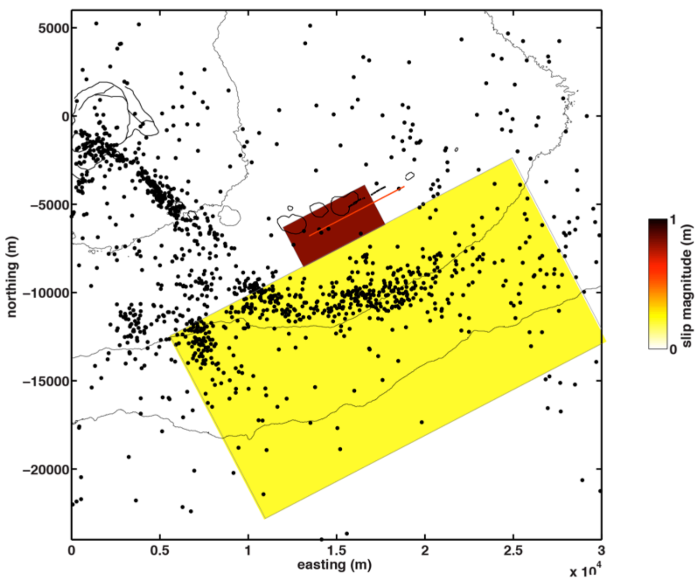

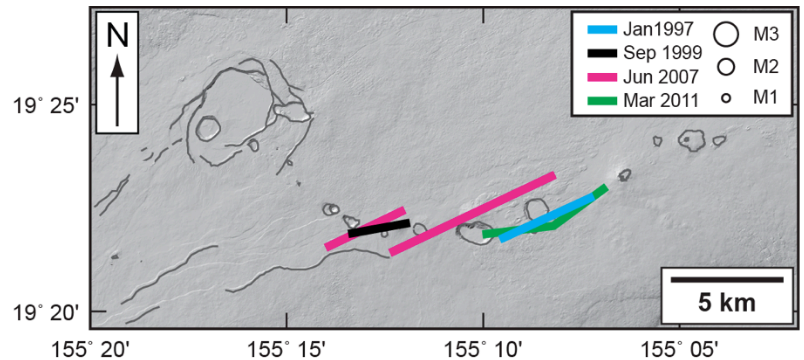

Surface traces of recent dikes (from M. Poland)

Models of 2011 and 1997 post-diking (Desmarais and Segall, 2007) are quite different, with the latter finding deeper (2-4 km) opening compared to both shallow dike opening and deep sill opening

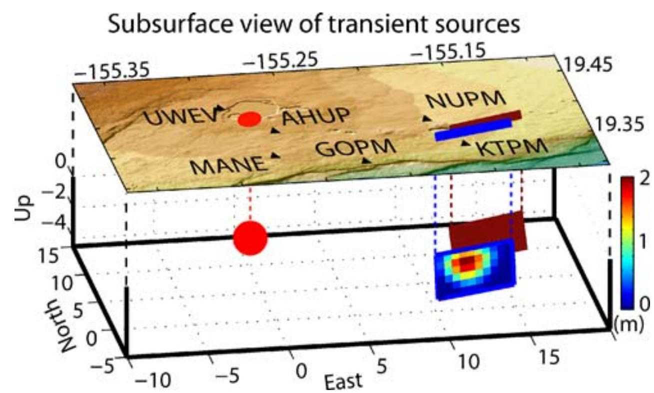

Fig. 5 Dike parallel cross section of both the 1.96 m uniformly opening 30 January 1997 intrusion dike and the cumulative distributed slip modeled in this study

Desmarais and Segall, 2007

UAVSAR
Uninhabited Aerial Vehicle Synthetic Aperture Radar

Future directions

UAVSAR needed for volcano rapid response:

- Need dense temporal sampling when system is most dynamic
- Need for low-latency data
- Need to characterize signals to drive models that will improve forecasts

Current efforts in the Pacific "Ring of Fire" are designed to lay the foundation for future volcano eruption response.

Need topographic change for effusive eruptions, including lava domes

Copahue Volcano, Southern Andes

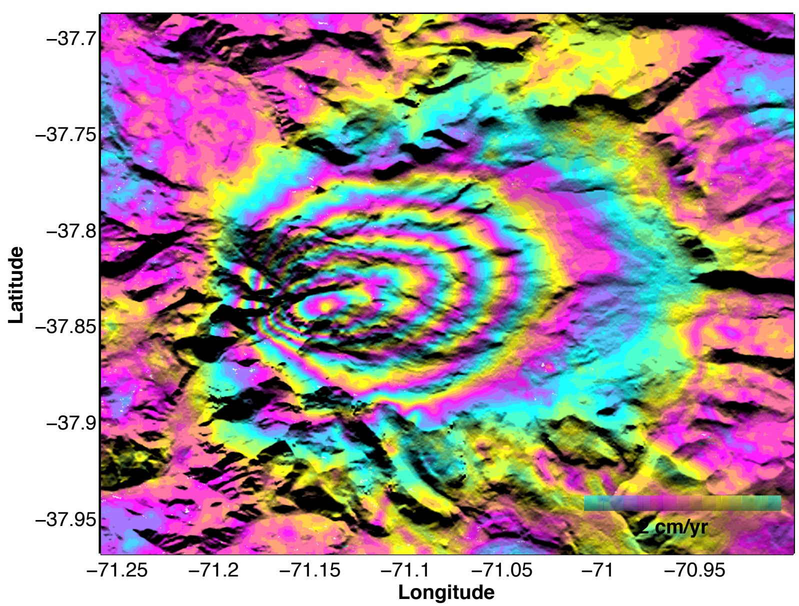

Mean velocity map for smoothed solution. Fringe rate is 2 cm/yr.

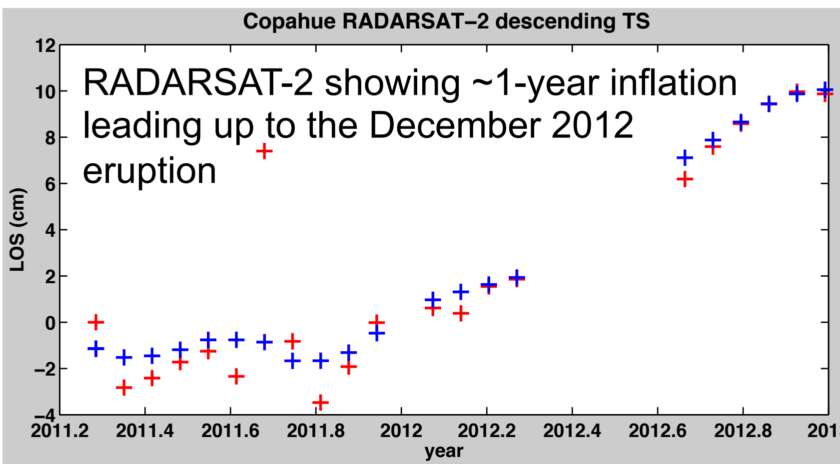

support

Red + raw InSAR TS for area of peak deformation; blue + smoothed TS.

RADARSAT-2 interferograms courtesy S. Samsonov, CSA; TS processing by P. Lundgren, JPL

UAVSAR
Uninhabited Aerial Vehicle Synthetic Aperture Radar

Kilauea: CSK time series

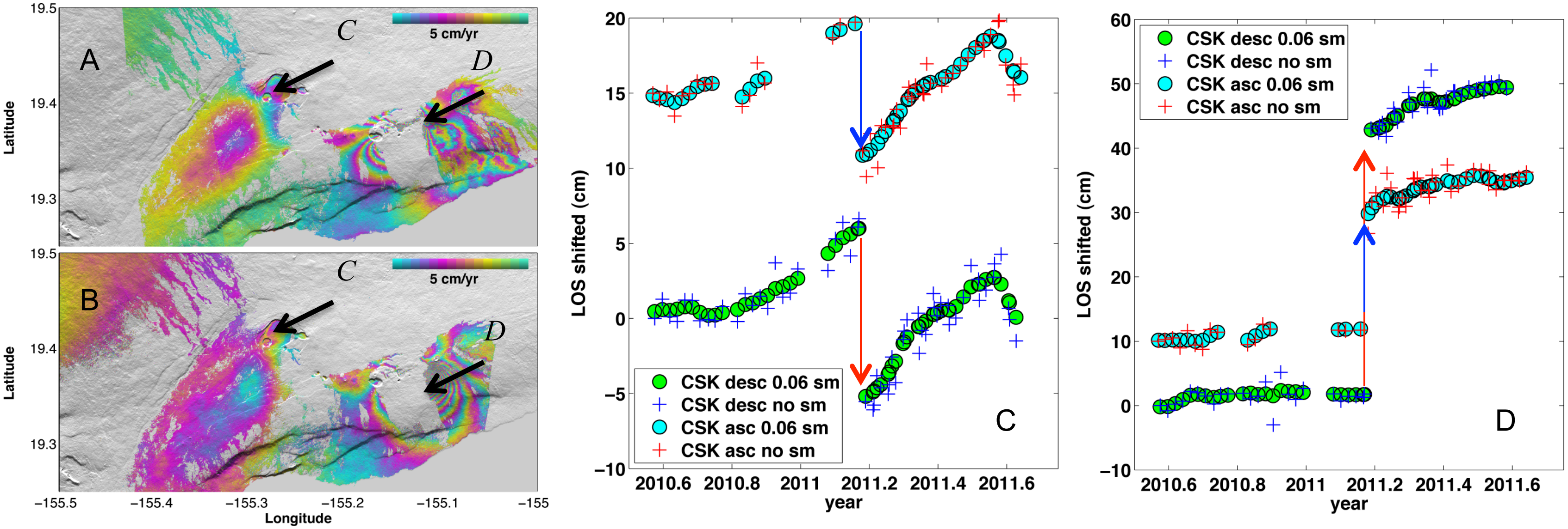

InSAR time series for one year (late July 2010 – August 2011) of COSMO-SkyMed data. (A) Ascending track mean velocity (5 cm/yr color cycle). Arrows indicate approximate locations of time series shown in (C) and (D). (B) Descending track mean velocity. (C) Point time series for Kilauea caldera and (D) for points near the Kamoamoa dike eruption. The March 2011 fissure eruption shows sharp deflation at Kilauea until mid-2011, whereas (D) shows post-dike transient. Plus (+) signs are unsmoothed time series, circles are time series with a temporal triangular filter width of 3 weeks. Ascending data time series are shifted relative to the descending data. *A* and *B* in (C) and (D) refer to series from (A) and (B).

Arrows show Kilauea summit deflation and ERZ opening due to March 2011 fissure eruption.

Pre-eruption deformation

UAVSAR
Uninhabited Aerial Vehicle Synthetic Aperture Radar

COSMO-SkyMed 4-months pre-Kamoamoa eruption

ascending 30/10/2010-27/02/2011 descending 10/11/2010-03/03/2011

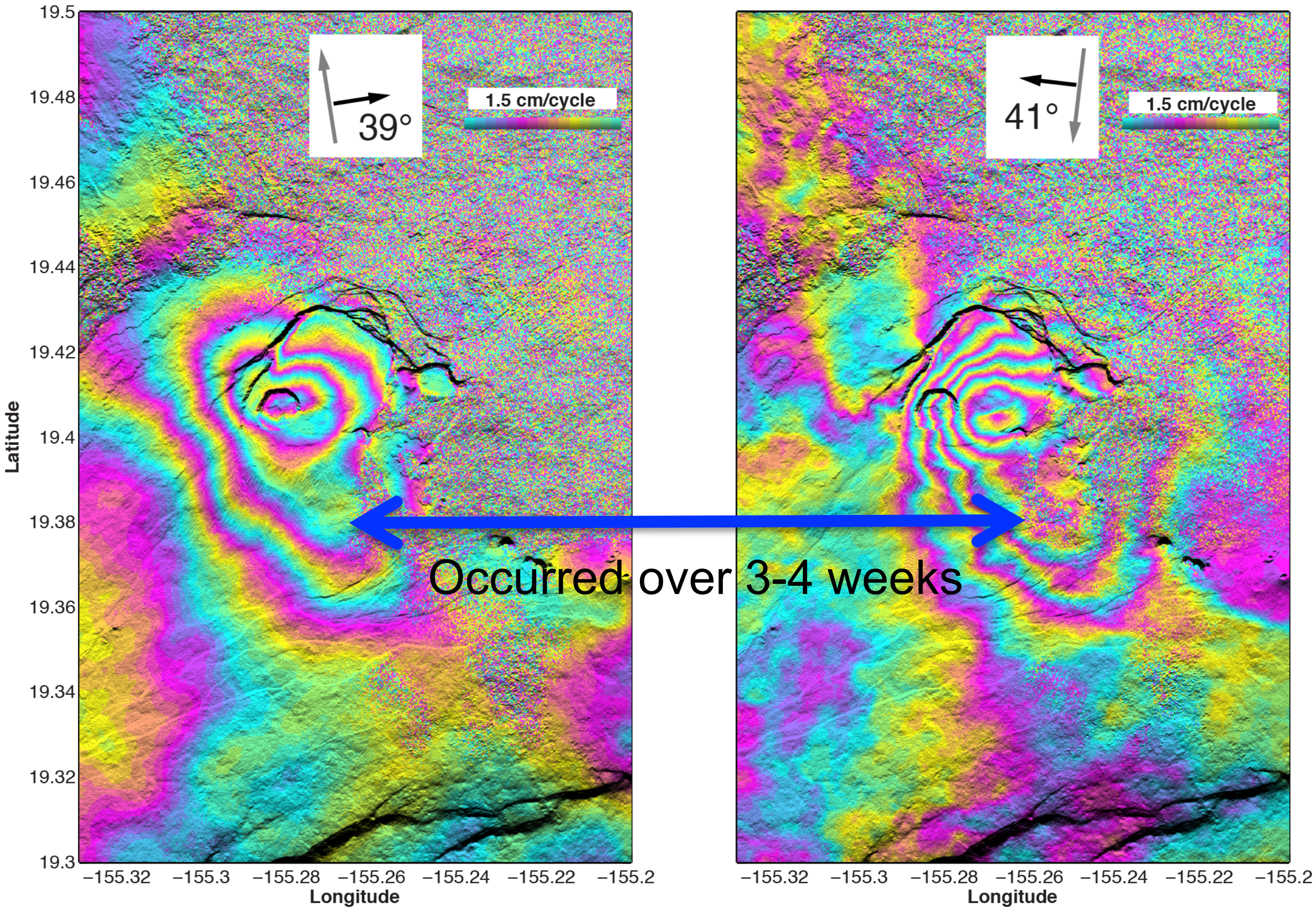

Precursory deformation south of Kilauea caldera in the 3 weeks prior the Kamoamoa eruption are several fringes at X-band and would only be about half a fringe at L-band.

Summary

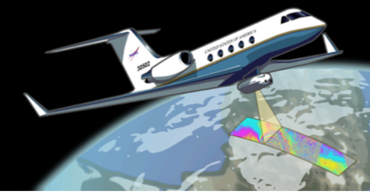

- UAVSAR applied to active volcanoes has been successful in constraining dike opening of the 2011 Kamoamoa eruption, Kilauea volcano, Hawaii.
- Post-diking deformation from multiple look directions from UAVSAR are important for constraining deep dike accommodation.
- Local deformation at volcanoes such as Pacaya Volcano, Guatemala, provide important insight into edifice deformation and slope hazard.
- Future repeat observations in Japan and South America expand background observations that will provide the basis for responding to future large eruptions in the Pacific Rim.

Acknowledgement: